Engineering 6 (2020) 621–636

Contents lists available at ScienceDirect

Engineering

journal homepage: www.elsevier.com/locate/eng

Research
Materials Genome Engineering—Review

State-of-the-Art Review of High-Throughput Statistical Spatial-Mapping Characterization Technology and Its Applications

Haizhou Wang [a,b], Lei Zhao [a,b,*], Yunhai Jia [b,c,*], Dongling Li [a,b], Lixia Yang [b], Yuhua Lu [b], Guang Feng [b], Weihao Wan [b]

[a] *Beijing Advanced Innovation Center for Materials Genome Engineering, Central Iron and Steel Research Institute, Beijing 100081, China*
[b] *Beijing Key Laboratory of Metal Materials Characterization, Central Iron and Steel Research Institute, Beijing 100081, China*
[c] *NCS Testing Technology Co., Ltd., Beijing 100081, China*

A R T I C L E I N F O

Article history:
Received 26 March 2019
Revised 18 November 2019
Accepted 11 May 2020
Available online 16 May 2020

Keywords:
Material heterogeneity
High-throughput characterization
Statistical spatial-mapping
Original-position statistical-distribution analysis

A B S T R A C T

Macroscopic materials are heterogeneous, multi-elementary, and complex. No material is homogeneous or isotropic at a certain small scale. Parts of the material that differ from one another can be termed "natural chips." At different spots on the material, the composition, structure, and properties vary slightly, and the combination of these slight differences establishes the overall material performance. This article presents a state-of-the-art review of research and applications of high-throughput statistical spatial-mapping characterization technology based on the intrinsic heterogeneity within materials. High-throughput statistical spatial-mapping uses a series of rapid characterization techniques for analysis from the macroscopic to the microscopic scale. Datasets of composition, structure, and properties at each location are obtained rapidly for practical sample sizes. Accurate positional coordinate information and references to a point-to-point correspondence are used to set up a database that contains spatial-mapping lattices. Based on material research and development design requirements, dataset spatial-mapping within required target intervals is selected from the database. Statistical analysis can be used to select a suitable design that better meets the targeted requirements. After repeated verification, genetic units that reflect the material properties are determined. By optimizing process parameters, the assembly of these genetic unit(s) is verified at the mesoscale, and quantitative correlations are established between the microscale, mesoscale, macroscale, practical sample, across-the-scale span composition, structure, and properties. The high-throughput statistical spatial-mapping characterization technology has been applied to numerous material systems, such as steels, superalloys, galvanization, and ferrosilicon alloys. This approach has guided the composition and the process optimization of various materials.

1. Introduction

In 1995, Xiang et al. [1] published research on a "combinatorial materials chip" as a cover article in *Science*. On one substrate, simultaneous integrated growth and characterization were achieved with 128 new materials with different components, and also high-throughput material screening was achieved, along with a systematic description of the "phase diagram of the material." Since then, similar high-throughput material syntheses and characterization technologies have been developed and applied in various fields. Examples include a "diffusion multiple approach" [2], used to accelerate the design of structural materials; high-throughput film-growth technology [3], used to screen semiconductor materials with discrete and continuous components; and an ink-jet delivery system, used to screen composite powders [4]. Other high-throughput experimental techniques include the rapid characterization of composition [5], structure [6], electrochemical properties [7], catalytic properties [8], electromagnetic properties [9], magnetic properties [10], optical properties [11], thermal properties [12], and mechanical properties [13]. The screening of unknown materials has been accelerated significantly, and work that took years with conventional methods can be achieved in

* Corresponding authors.
E-mail addresses: zhaolei@ncschina.com (L. Zhao), jiayunhai@ncschina.com (Y. Jia).

https://doi.org/10.1016/j.eng.2020.05.005

one week with high-throughput characterization technology, resulting in revolutionary breakthroughs. Nevertheless, the "combinatorial materials chip" technology has shortcomings; chip preparation often differs significantly from the actual material production, which suggests that significant effort is still required to scale up production to enable the transfer from laboratory to application. Wang et al. [14,15] proposed a high-throughput statistical spatial-mapping characterization technology based on original-position statistical-distribution analysis (OPA). Based on a recognition of the intrinsic material heterogeneity, the proposed technique carried out high-throughput and across-scale span statistical-distribution characterization of samples. Massive datasets were acquired promptly with an exact location correspondence between macroscopic, mesoscopic, and microscopic composition, structure, and properties. A spatial-mapping relationship between datasets was established so that a correlation was obtained between the composition, structure, and properties. Genetic units with superior performance were screened rapidly and selected to guide the modification of existing materials and for production optimization. Through machine learning of massive spatial-mapping datasets, these screened genetic units could be reconstructed reversely "bottom up" from the microscale to the macroscale, so that an optimum combination of composition, structure, and properties could be achieved at the macroscopic level. Thus, a reverse design of new materials could be accomplished and accelerated. Therefore, an intrinsically heterogeneous actual material is also considered a "natural chip" with various combinations. Because this kind of "natural chip" originates from an actual production process, it has special significance in guiding the modification of existing materials and the optimization of the production process.

2. High-throughput statistical spatial-mapping characterization technology

2.1. Intrinsic material heterogeneity

Macroscopic materials are heterogeneous, multi-elementary, and complex. No material is homogeneous or isotropic at a certain small scale. Parts of the material that differ from one another can be termed "natural chips." At different spots of the material, the composition, structure, and properties vary slightly, and the combination of these slight differences establishes the overall material performance. Like human genes, a material has a smallest unit of matter, which is a genetic unit and reflects the material properties. The genetic units vary for different materials, and could be a natural atom, molecule, or ion that makes up a substance, phases, clusters, functional groups, units, or grains formed by a combination of these particles. Certain processes or technologies can be used to combine the same or different genetic units into "genomes" or even into final materials with certain properties. This combinatorial process or technology can be referred to as an "assembly." Because of the complexity and diversity of the different materials and processes, the "assembly" of genetic units is diverse. Research into materials genome engineering includes high-throughput synthesis, characterization, screening, assembly, and repeated verification of target genetic units that are designed on demand. Thus, a correlation can be established between the microscale, mesoscale, macroscale, and across-scale span, as well as the composition, structure, and properties, to guide the research and development of new materials and the modification of existing materials with less time and cost. Wang et al. [16] used OPA characterization technology to study the distribution of Nb in the disk forging of a superalloy compressor. Nb was distributed unevenly in the cold-die-affected area on the lower die and in the center of the forging, which led to a failure of the disk forging. Through results analysis, uneven parts were removed in the process, which raised the final product quality to standard. The physical properties of amorphous alloys in different directions are the same, because their atomic structures are amorphous and isotropic at the macroscopic scale. Many studies have shown that the static structure and dynamics of amorphous alloys at the nanoscale or microscale are heterogeneous [17–24]. Therefore, the material heterogeneity should be acknowledged. However, if genetic units of material could be identified more clearly based on their intrinsically heterogeneous nature, faster and better designs and the development of new materials with improved properties could be achieved.

2.2. The high-throughput statistical spatial-mapping characterization technology

High-throughput statistical spatial-mapping characterization is based on the intrinsic material heterogeneity. Through the across-scale span characterization of a material, different compositions, structures, and properties are acquired from tens of thousands of material microarrays. A statistical spatial-mapping model between the sets of parameters is established based on the original material position. By using high-throughput computations, databases can be formed by screening genetic units, which determines the screened material properties and forms a database of material with the help of high-throughput computations. Materials-design optimization is carried out to guide material modification, process optimization, and the discovery of new materials, as shown in Fig. 1.

The high-throughput statistical spatial-mapping characterization process is shown in Fig. 2, and uses a series of rapid characterization techniques to analyze the across-scale span from the macroscale to the microscale. Datasets of composition, structure, and properties at each location are acquired rapidly for practical sample sizes. Through accurate positional coordinate information, and with reference to a point-to-point correspondence, the database is set up to contain spatial-mapping lattices. The design requirements of the research and development of materials are used to select spatial-mapping datasets within the required target intervals from the database. Statistical analyses, including statistical frequency within the range of parameters, statistical correlation between parameters, statistical elimination of the outliers, reasonable criteria, and models, can be used to select the design that best meets the targeted requirements. After repeated verification, genetic units that reflect the material properties are determined. Established pointing parameters in the process optimization are used to verify the assembly of these genetic units on the mesoscale, and quantitative correlations are established between the microscale, mesoscale, macroscale, practical sample, across-scale span composition, structure, and properties.

High-throughput statistical spatial-mapping characterization is like walking through a maze. By using the multi-path parallel trial method, the efficiency of discovering new materials can be improved significantly. The research and development single trial-and-error mode that was applied to existing materials can be discarded, and a new approach for the rapid research and development of new materials is presented. An innovation system for material research and development is constructed herein, which involves a "high-throughput trial-and-error method" that reduces the cost and shortens the research and development cycle for new materials.

2.3. Across-scale span original-position statistical-distribution analysis

OPA is a technology that performs a quantitative statistical-distribution analysis of chemical composition and morphology at

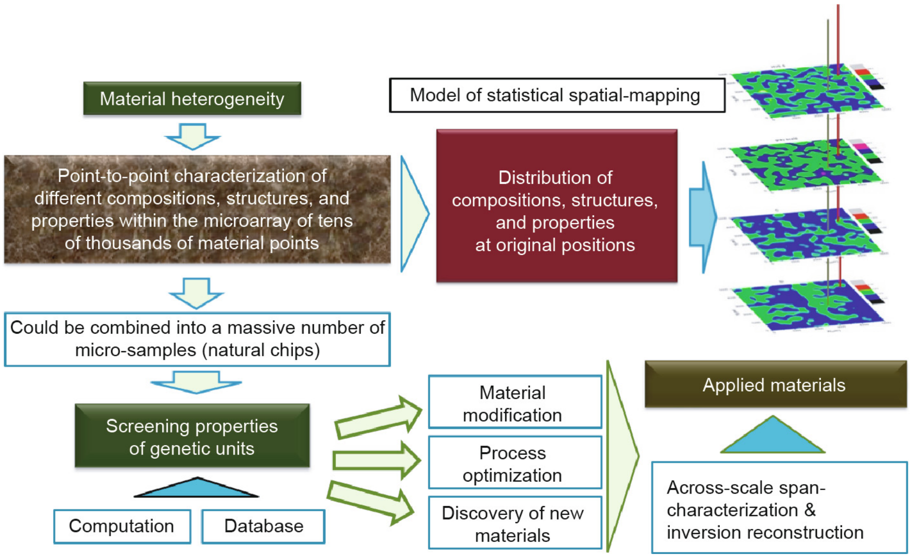

Fig. 1. Combined technology of microarray statistical spatial-mapping based on material heterogeneity.

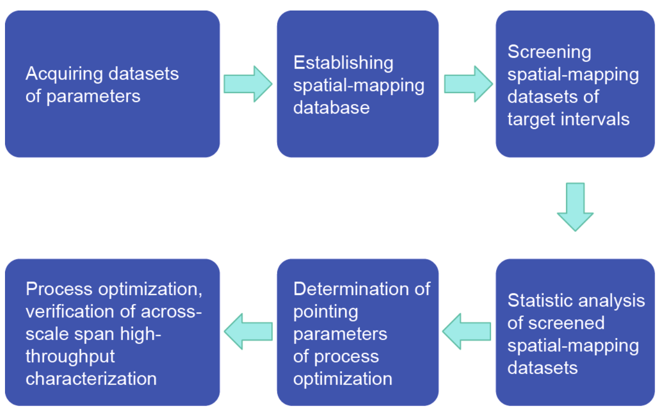

Fig. 2. Process of characterization of high-throughput statistical mapping.

the macroscopic scale (cm^2). This analysis uses the location distribution information of chemical composition, content distribution statistical information, and state-distribution statistical information. The information can be divided into one-, two-, and three-dimensional OPA based on a regional division [25–32]. OPA technology has been applied to characterize composition, structure, and mechanical properties. Advanced technologies have been developed, such as Spark-OPA, laser-induced breakdown spectroscopy (LIBS)-OPA, laser-ablation (LA) inductively coupled plasma mass spectrometry (LA-OPA), micro-X-ray fluorescence (μXRF) OPA, full-view-metallography (FVM)-OPA, macroscopic scanning-electron microscopy (SEM)-OPA, and fluid microprobe-OPA. A series of instruments and devices with independent intellectual property rights has also been developed.

2.3.1. Spark-OPA

As the main means to characterize the macroscopic statistical distribution of materials, Spark-OPA technology was developed from the optical emission spectroscopy (OES). Traditional OES pre-sparks the sample and integrates the signals in order to acquire reliable results, but this method cannot analyze the original inclusions information, since the inclusions have been remelted by the pre-spark. Spark-OPA derives a series of technologies including single-spark discharge, signal-resolution extraction, non-pre-spark continuous excitation, and synchronous-scanning positioning, by which millions of pieces of data on the original content and state information of each element are obtained to correspond to their original positions within the material. Statistical analysis is used to quantitatively characterize parameters such as segregation, looseness, and the inclusion distribution of materials. A single-spark discharge can be regarded as a kind of unconstrained probe with a size of 1–10 μm, and a spark point contains millions of these probes. Thus, Spark-OPA can provide accurate information on the position distribution, state distribution, and quantitative distribution of each component on a macroscopic scale (hundreds of square centimetres) [33]. Spark-OPA is an across-scale span-characterization technology that could reflect the microstate at the macroscale. The original-position metal analyzer OPA-100 was developed in 2002, with seven associated patents [34–40], and was awarded the second-place prize at the Chinese National Technological Invention in 2008 [41]. It has been upgraded to a fourth-generation product (as shown in Fig. S1 in Appendix A).

Spark-OPA technology has been developed into a mature commercial application for composition segregation and the quantitative characterization of inclusions in macroscopic metal samples. This technology has played an important role in guiding production optimization. Compositional segregation characterization has been applied to the characterization of carbon steel and stainless steel materials, such as continuously cast bloom, cord steel, and ship plate steel [42–81]. For example, Li et al. [82] studied the round billet of No. 35 carbon steel and found a bright white band at the edge of the billet that was produced by electromagnetic stirring; an obvious negative segregation of elemental C, Si, Mn, and P was the main reason for the uneven distribution of grain structure and Vickers hardness (HV) (Fig. 3). The composition segregation and quality defects both have been explored in detail for nonferrous metals such as aluminum alloys and brass, etc. [83–85].

For the quantitative characterization of inclusions, Wang's research team [86–89] established an analytical method for the content and size distribution of inclusions, such as Mn, Al, Ti, and Si in steel, through the statistical analysis of several abnormal sparks in a single discharge. Spark-OPA technology has been applied to the statistical distribution analysis of inclusions in various metal materials, such as carbon steel, stainless steel, heavy rail steel, beam steel, gear steel, and high-pressure boiler-tube steel [90–107]. For example, Luo et al. [108] used Spark-OPA technology to conduct a full-scale characterization of the cross-section of a

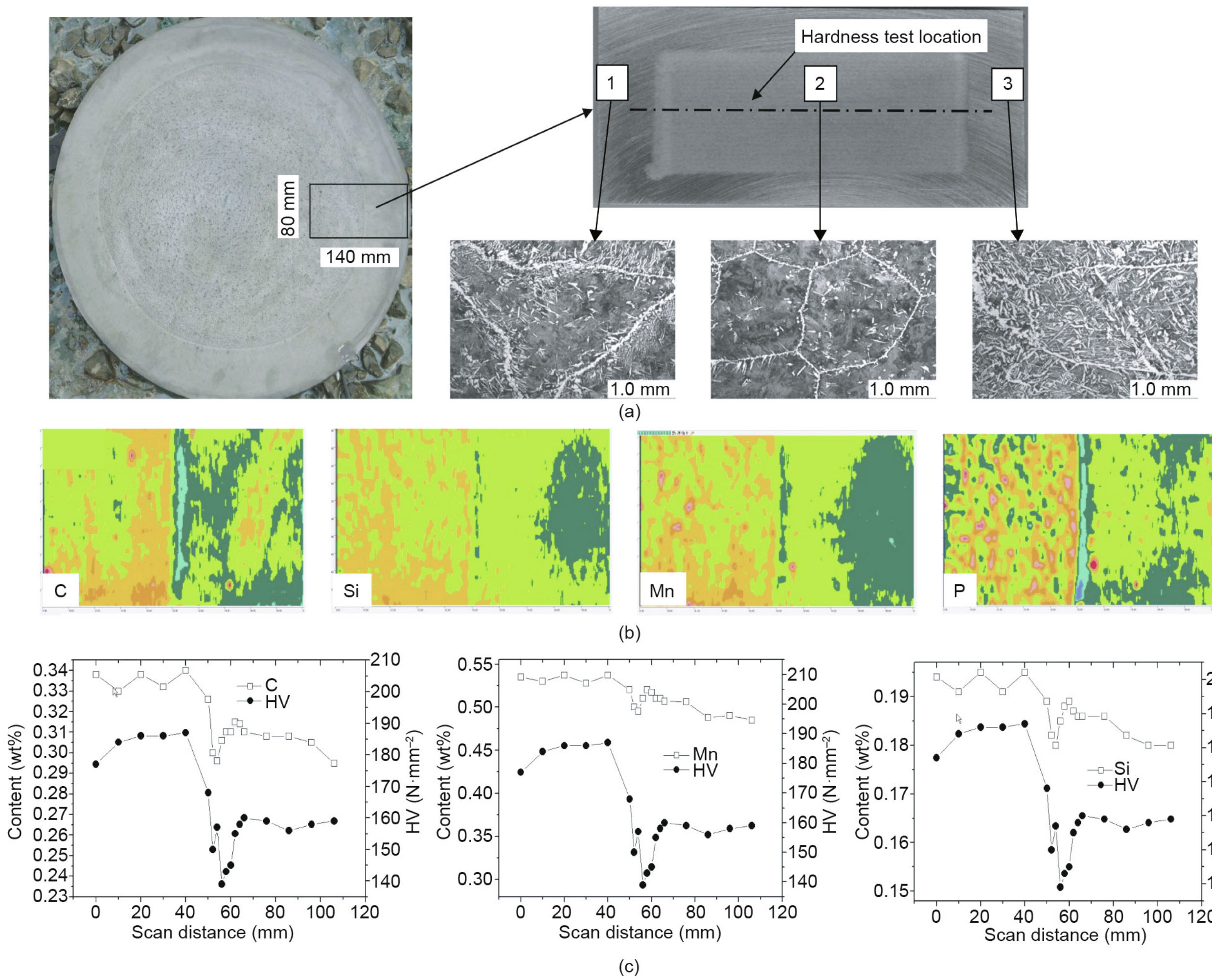

Fig. 3. Application of Spark-OPA technology in the composition segregation of an electromagnetically stirred round billet [82]. (a) Analyzed region (106 mm × 52 mm); (b) two-dimensional elemental distribution in the analyzed region; (c) relationship between composition distribution and HV of C, Mn, and Si.

continuously cast plate of stainless steel (Samples A–N) and found that, in the macroscopic test, the proportion of Al–Ca inclusions and that of small-particle inclusions were slightly higher at the edge of the white band. The proportion of Al–O inclusions and that of large-particle inclusions were slightly higher in the central region, which was consistent with the SEM analysis. An edge-to-center distribution of aluminum inclusions was obtained in the sample (as shown in Fig. 4).

2.3.2. LIBS-OPA

LIBS-OPA technology is based on a quantitative analysis of the spectrum signal of the atomic emission that is generated by the action of a high-energy laser beam on the material surface. The beam spot is micron-to-millimeter sized. This technology provides the advantages of non-contact analysis, micro-area analysis, and in-depth analysis, with point and line scanning. One-dimensional depth analysis and two-dimensional surface analysis enable a fine positioning of the sample surface and are an effective means of mesoscopic-to-macroscopic across-scale span materials characterization [109–111]. The first commercial LIBS-OPA100 was developed in 2010, with several associated patents [112–115]. It has since been upgraded to a second-generation product (Fig. S2).

LIBS-OPA technology has advantages in the characterization of composition segregation of small samples. Therefore, LIBS-OPA100 have been widely used to analyze the distribution of various components in small samples, such as medium- and low-alloy steel plate, cord wire rod, the surfacing fusion zone of X80 pipeline steel, and electromigration gadolinium rods [116–122]. Their work helped to pinpoint existing problems in production through the characterization of composition segregation. Fig. 5 shows a LIBS-OPA characterization of the composition distribution and a study of the relevance between the microstructure and the microscopic distribution of HV in the surfacing zone of X80 pipeline steel.

Many studies have been carried out with LIBS-OPA technology on the analysis of sample defects. Various shape defects on the surface of auto and cold-rolled hot-galvanized sheets were tested by LIBS-OPA100 with modes of line scanning, surface scanning, and depth analysis, respectively [123–126]. The results showed that defects were accompanied by elemental segregation, most of which were caused by the introduction of mold powder into the production. Their research was significant in guiding improvements in coated-sheet production. Fig. 6 shows an in-depth and line-scanning study of the defects of an auto sheet.

In recent years, LIBS-OPA technology has progressed to inclusion analysis. Yang et al. [127–130] found that the number of abnormal signals in the laser spectrum reflected the number of inclusions, and that the intensity of the abnormal signals was related to the size of the inclusions. They used this information to analyze the contents of acid-insoluble aluminum, MnS inclusions, and Si–Al–Ca–Mg composite inclusions in steel. The results of their analysis agreed with those of traditional wet-chemical analysis. Fig. 7 depicts a study of the LIBS-OPA quantification of MnS inclusions.

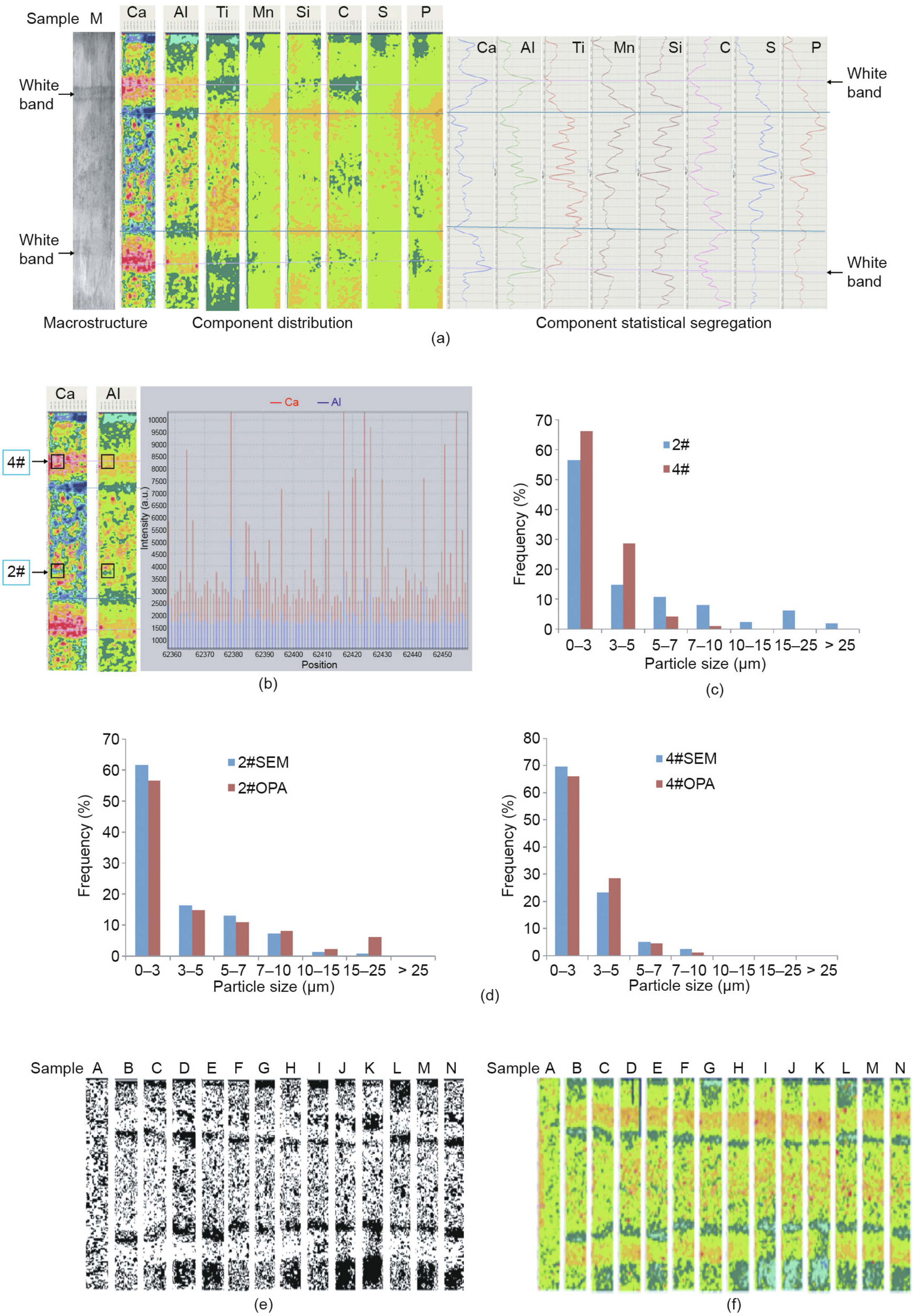

Fig. 4. Application of Spark-OPA in the characterization of inclusions in continuously cast steel plate [108]. (a) Analysis of low-magnification component distribution and statistical segregation of sample M; (b) diagram of abnormal spark channels for Al and Ca; (c) bar graph of Al particle-size distribution inclusions in regions 2 and 4; (d) bar graphs of particle-size distribution of Al inclusions in regions 2 and 4 by SEM and OPA; (e) distribution of Al inclusions in the plate; (f) distribution of elemental composition of Al in the plate.

2.3.3. LA-OPA

The principle of LA-OPA technology is that the sample can be stripped and gasified layer by layer by a microbeam-focused laser, transferred to an inductively coupled plasma (ICP) source, be ionized or atomized in an inert gas environment as an aerosol, and be analyzed quantitatively by mass spectrometry. The laser-beam spot of this technology is on the order of microns, with a low detection limit and a high sensitivity, and is suitable for the statistical

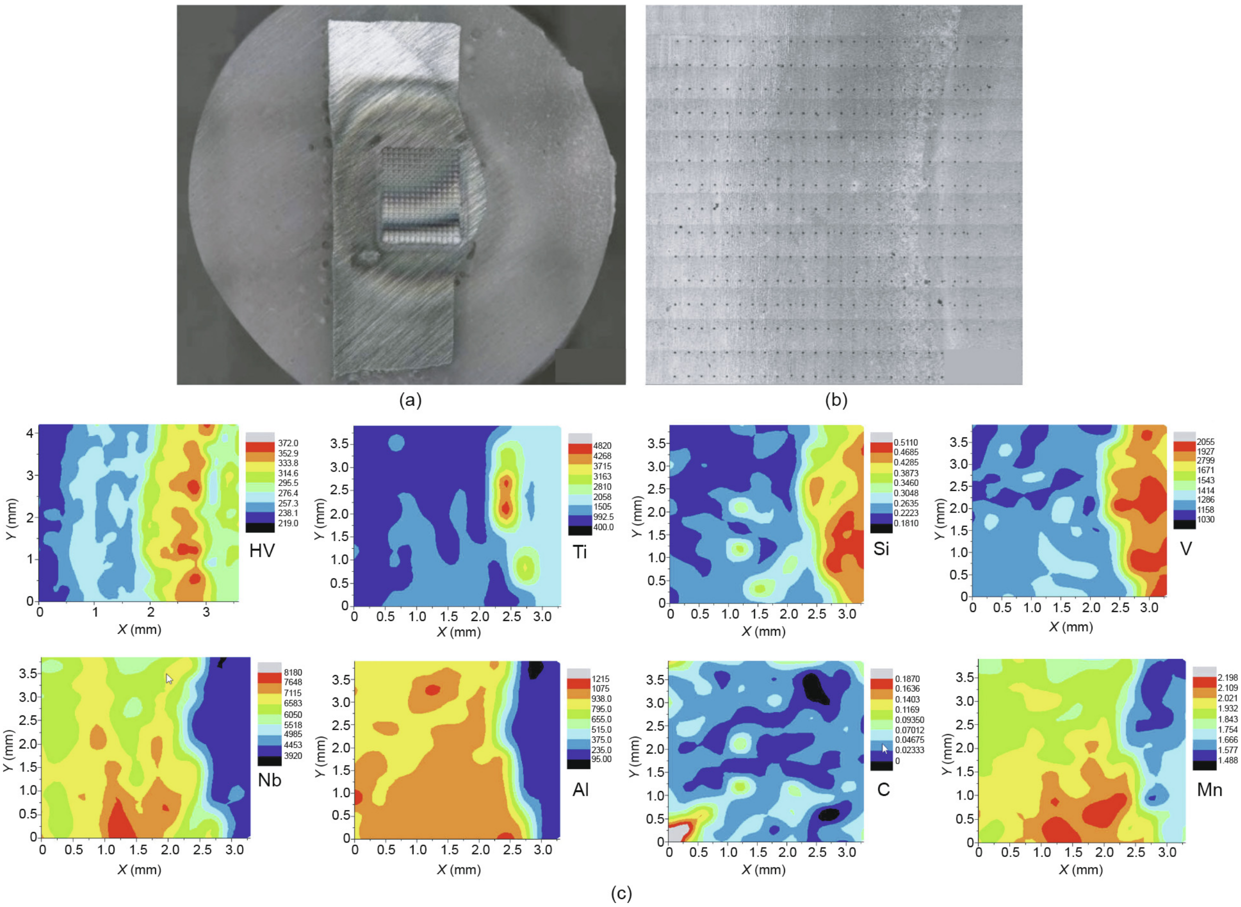

Fig. 5. LIBS-OPA characterization, microstructure, and microscopic distribution of HV in the surfacing zone of X80 pipeline steel [116]. (a) Scanning area of the surfacing zone of X80 pipeline steel (3.3 mm × 3.9 mm); (b) full-view microstructure and microscopic distribution of HV; (c) microscopic distribution of HV and composition in the surfacing zone.

analysis of the surface distribution of low-content and trace components in hetero-morphed or small samples. This technique provides another effective means of mesoscopic-to-macroscopic across-scale span material characterization. In 2008, the LA-OPA technology has been developed and applied to the statistical-distribution characterization of various hetero-morphed surfaces of small samples, such as spherical flat steel, galvanized steel pipes, welded pipes, superalloy turbine blades, dysprosium bars, pipeline steel cracks, and impact fractures [131–147]. They focused on the position distribution, statistical segregation, and maximum segregation of components; the relevance between these properties; and the material quality. In 2015, commercialization of the proprietary intellectual property rights was achieved for the LA-OPA characterization equipment (including a laser-ablation sampling device and an inductively coupled plasma mass spectrometer), as shown in Fig. S3. Two patents were applied for Refs. [148,149], and the Beijing Conference and Exhibition on Instrumental Analysis (BCEIA) Gold Prize established by the China Association for Instrumental Analysis was won in 2015. Fig. S4 shows the statistical-distribution characterization of directionally solidified superalloy turbine blades by LA-OPA technology; the precipitation of elements with low melting points in the polycrystalline zone resulted in blade defects [150].

2.3.4. μXRF-OPA

μXRF-OPA technology focuses X-rays into a small beam with a diameter of about 20 μm by using capillary lenses. The chemical compositions on the material surface can be detected by non-destructive surface scanning by μXRF-OPA, and statistical-distribution analysis is conducted on the large acquired dataset. μXRF-OPA technology is a non-destructive testing method with improved resolution but a low fluorescence-intensity loss, which enables a scanning range up to centimeters and provides an efficient method for characterizing materials from the mesoscale to the macroscale. In 2017, a prototype with proprietary intellectual property rights was developed, as shown in Fig. S5. Yang et al. [151] conducted statistical-distribution characterization of the composition segregation in microregions of weatherproof steel sheets with μXRF-OPA technology. The results showed that the segregation of Ti, Mn, P, and S in the fractured zone may be the main cause of cracking, as shown in Fig. 8. Li et al. [152] conducted statistical-distribution characterization of superalloy compositions that were produced by different processes with μXRF-OPA technology. Heat treatment improved the distribution uniformity of elemental Nb, Ti, Mo, and W, and the maximum segregation decreased significantly, as shown in Fig. 9.

2.3.5. FVM-OPA

FVM-OPA technology, which is based on full-automatic scanning metalloscopy, rapidly acquires an atlas of the metallographic structure and position information of the entire sample surface, and then pieces data into a complete image with precise location information. Through a statistical analysis of the original digital signal (gray value) at each pixel in the image, automatic

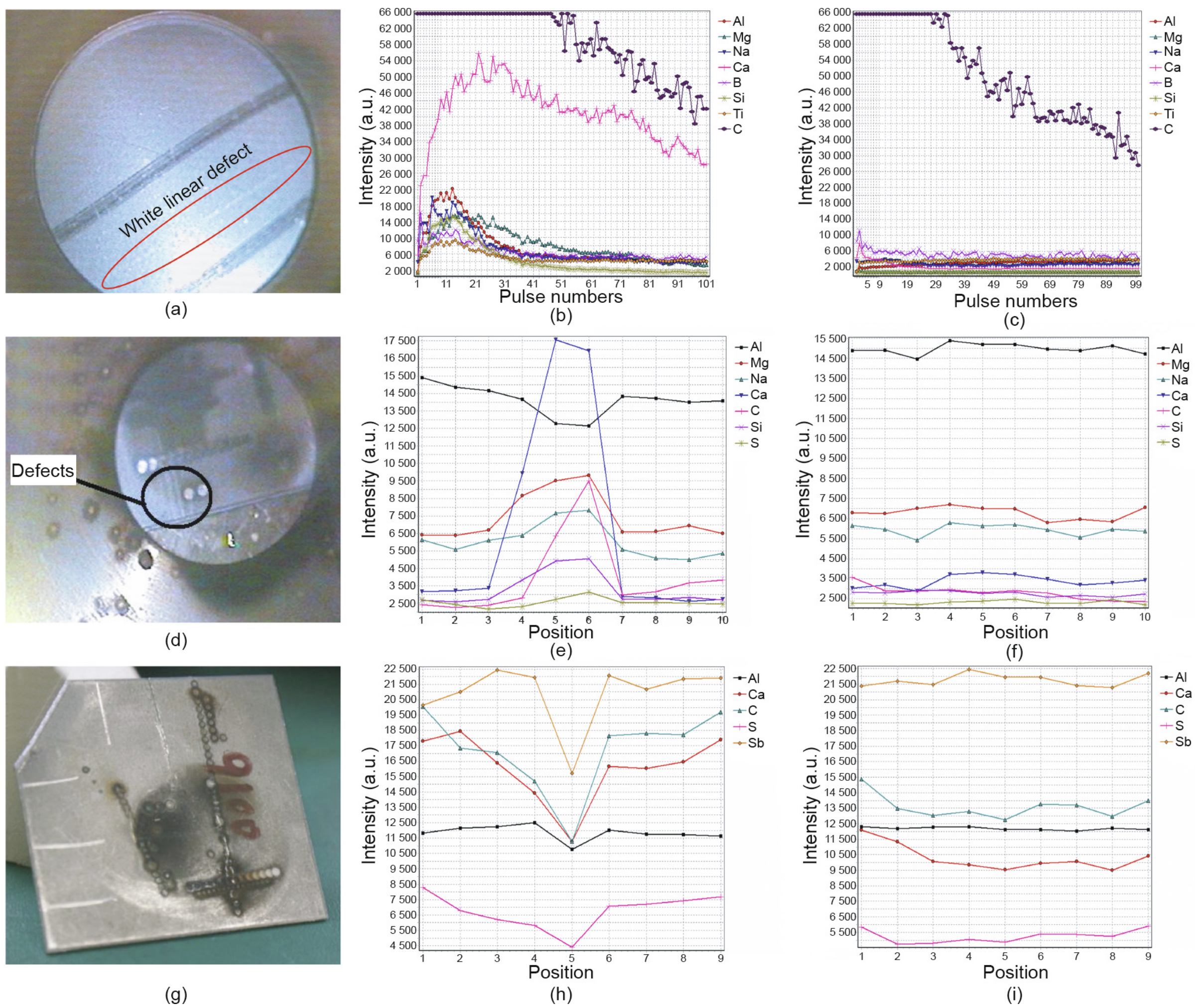

Fig. 6. In-depth and line-scanning study of the defects of an auto sheet with LIBS-OPA technology [125]. (a) Line defect of a galvanized sheet; (b) depth analysis of the defect; (c) depth analysis of non-defect spots; (d) band defects of an auto sheet; (e) line scanning of surface defects; (f) line scanning of surface non-defect spots; (g) a scratch defect and artificial defects on an auto sheet; (h) line scanning of scratch defects; (i) line scanning of artificial defects.

identification and quantitative statistical-distribution characterization are achieved for various structural property types (e.g., looseness, cracks, shrinkage cavities, defects, crystalline grains, precipitated phases, and inclusions). Through statistical analysis of the structural orientation in the entire sample range, FVM-OPA technology resolves the issues of subjectivity, randomness, and contingency when artificially selecting the field of view, which results in a more comprehensive characterization of the metallographic structure. Wang et al. [153] conducted statistical-distribution analyses of martensite and ferrite in a ferrosilicon alloy by FVM-OPA technology. The gray value of the structure was quantitatively correlated with the C content, Si content, C/Si ratio, and HV (Fig. S6).

2.3.6. Macroscopic SEM-OPA

SEM-OPA technology uses an electron source with a high brightness and field-emission, high-resolution electromagnetic compound objective lens, and direct electron detector to achieve the high-throughput acquisition of images in macroscopic samples. The scanning time of an image of the same quality is 1/50th that of traditional SEM. Intelligent software integrates professional image libraries of a wide variety of specific materials, and automatically acquires and calibrates the category and characteristics of the observed structures. Graphic processor unit multi-threaded parallel computing and large data mining are used to conduct a more comprehensive statistical analysis of the overall distribution of the structural parameters of the macroscopic samples and to establish an improved statistical mapping correlation with the distribution of the composition and performance. Wang et al. [154] characterized a 12 mm diameter sample of nickel (Ni)-based single-crystal superalloy by SEM-OPA technology and obtained full-view surface-distribution information of the γ' phase, as shown in Fig. 10. The results showed that small γ'-phase grains were mainly distributed in dendritic stems while larger γ'-phase grains occurred between dendrites, as shown in Fig. 11.

2.3.7. Fluid-microprobe-OPA

Fluid-microprobe-OPA technology is based on the principle of isostatic pressure. Under the action of a high-pressure fluid (gas or liquid), because of the heterogeneous nature of the sample, the positions of different structures yield different deformations. By establishing a correlation between the micro deformations at each position and structure, a statistical distribution of the stress and strain at an original position is achieved. Fluid can be regarded as a continuously distributed and uniformly pressed microprobe. Therefore, fluid-microprobe-OPA technology performs, in a real sense, a continuous across-scale span, from nanometer to centimeter, and provides a high-throughput characterization of the

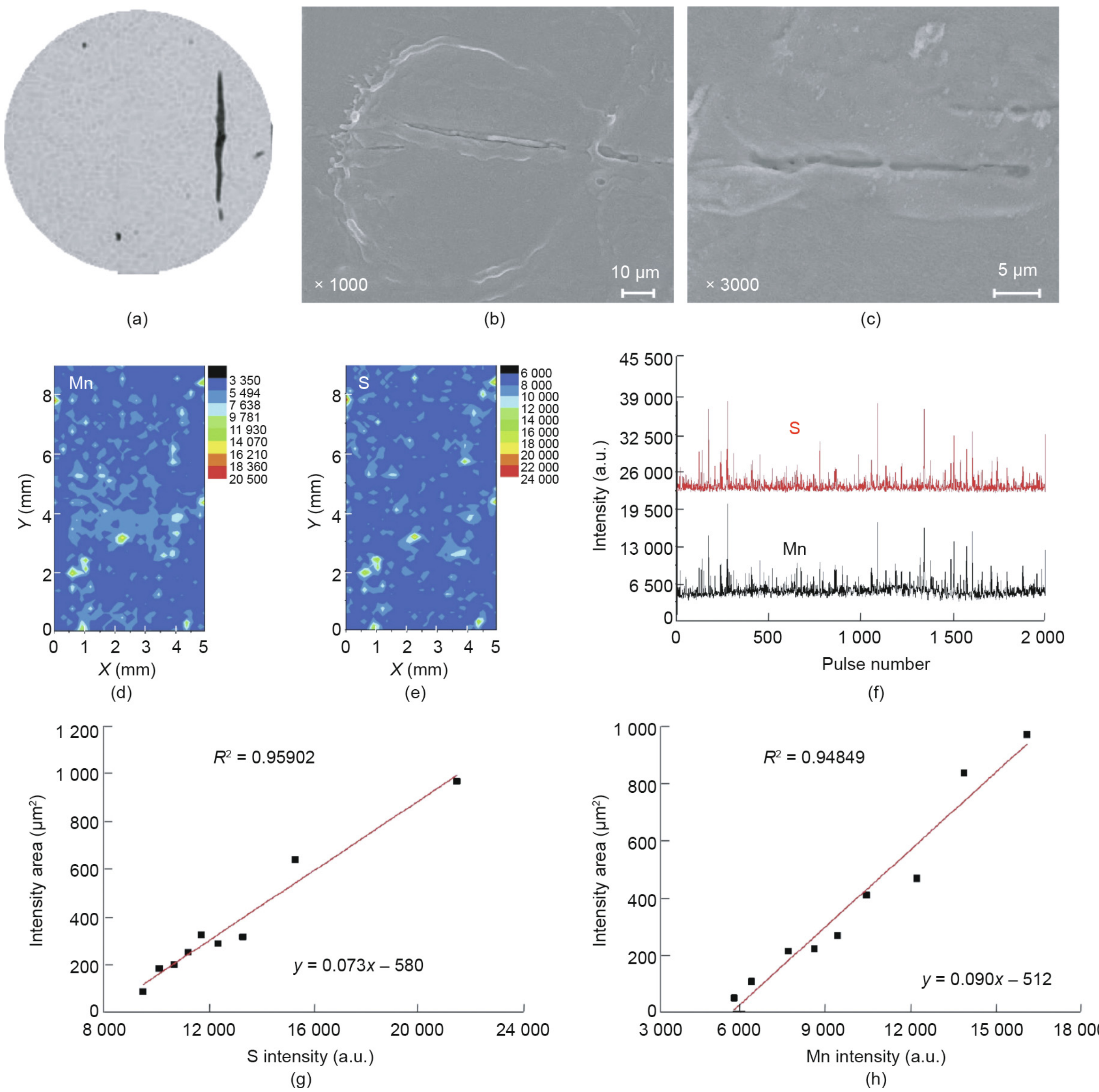

Fig. 7. LIBS-OPA study on MnS inclusions [128]. (a) MnS inclusions; (b) partially burnt inclusions; (c) completely burnt inclusions; (d) intensity distribution of Mn; (e) intensity distribution of S; (f) intensity of S and Mn; (g) linear fitting relation of the intensity of S and the area of inclusions; (h) linear fitting relation of the intensity of Mn and the area of inclusions.

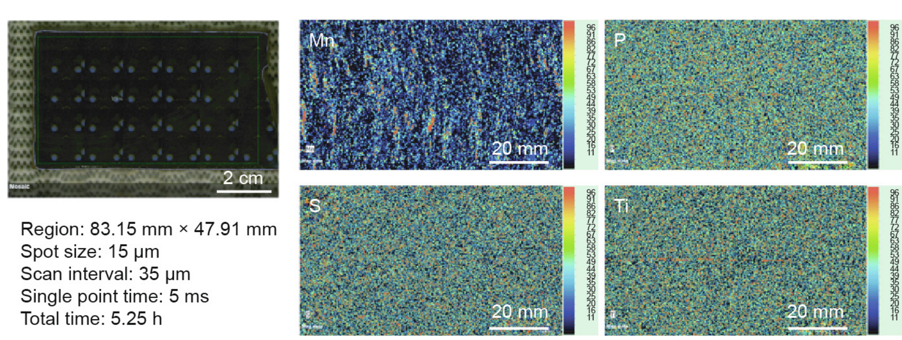

Fig. 8. Statistical-distribution characterization of composition segregation in microregions of weatherproof steel sheet [151].

mechanical properties. Feng et al. [155] studied the surface deformation, structural distribution, and HV of samples of high-chromium (Cr) white cast iron using fluid-microprobe-OPA technology. The deformation was related closely to the elastic modulus, equivalent modulus, and hardness, as shown in Fig. 12.

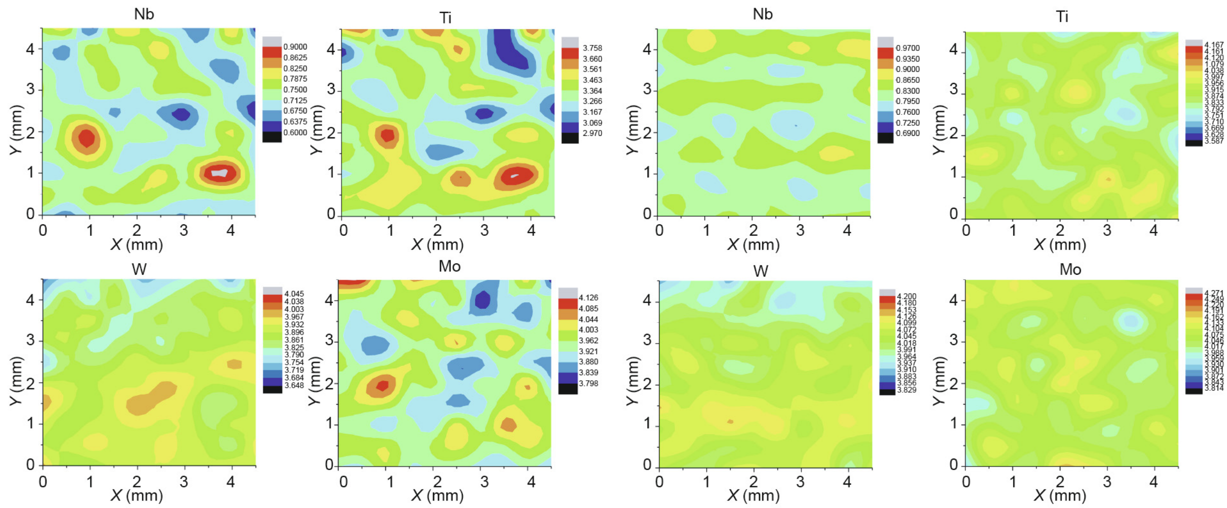

(a) (b)

Element (casting)	Average content (%)	RSD (%)	Maximum segregation degree
Nb	0.728	7.71	1.24
Ti	3.346	5.00	1.12
Mo	3.951	1.60	1.04
W	3.882	1.52	1.03

Element (heat treatment)	Average content (%)	RSD (%)	Maximum segregation degree
Nb	0.824	3.37	1.08
Ti	3.873	2.01	1.05
Mo	4.066	1.12	1.03
W	4.034	1.32	1.02

(c)

Fig. 9. Statistical-distribution characterization of the elements Nb, Ti, Mo, and W in superalloys produced by different processes [152]. (a) Cast; (b) heat treatment; (c) comparison of statistical components distribution. RSD: relative standard deviation.

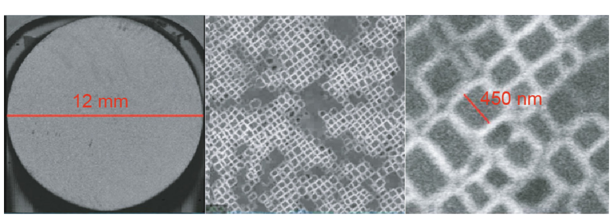

Fig. 10. Full-view and magnified γ'-phase crystal superalloy [154].

3. Demonstrative application of high-throughput statistical spatial-mapping characterization technology

3.1. Statistical spatial-mapping characterization of copper in the aging of G115 heat-resistant steel for ultra-supercritical power-generation units

Ultra-supercritical coal-fired power generation is an important measure to achieve energy conservation and emissions reduction. Research and development of heat-resistant materials is the greatest bottleneck restricting the development of advanced ultra-supercritical thermal-power units. G115 martensitic heat-resistant steel is developed based on existing 9 wt%–12 wt% Cr heat-resistant steel. Its ultimate service temperature exceeds 650 °C, which is of great engineering significance. G115 steel strengthens precipitation by 1.0 wt% copper (Cu) addition in the alloy design. Because of difficulties in the characterization of the precipitated Cu phase in martensitic steel, the form of existence, distribution, and strengthening mechanism of Cu in G115 steel is still unclear. Yang [156] used μXRF-OPA technology to conduct mesoscopic-to-macroscopic across-scale span characterization of a full sample surface (8.1 mm × 8.1 mm). A two-dimensional distribution of the intensity shows that elements were distributed uniformly in a mesoscopic state without obvious segregation, which indicates that the microbeam-fluorescence resolution was insufficient to characterize the discrepancy between the Cu in the sample (Fig. 13). SEM-energy dispersive spectroscopy (EDS) was used to locate the region with the highest intensity in microbeam-fluorescence analysis. At a 1000× magnification, because of the relatively low spatial resolution, elements in the region of characterization (300 μm × 300 μm) were in a relatively evenly dispersed state (Fig. 14). A white boxed area with slightly enriched Cu in the image was selected for microscopic characterization at a 20 000× magnification. Genetic units that contained Cu could be screened rapidly in this region (15 μm × 15 μm). The surface distribution of the energy spectrum showed that Cu-enriched areas were distributed at the interface or grain boundary, whereas other elements were negatively segregated, which indicates that Cu existed separately at the interface or grain boundary in the Cu-rich particles and did not form phases with other elements (Fig. 15). To determine the form of the Cu-rich particles, scanning transmission electron microscopy (STEM) was used to characterize the interfacial region (3 μm × 3 μm) in the thin area of the sample. Cu-rich particles in G115 steel formed a face-centered cubic-structured Cu-rich phase, which contained about 90.28 wt% Cu (Table 1). The particles were elliptical or spherical with an equivalent diameter of 50–242 nm and an average diameter of 114 nm. They often coexisted with M23C6 and Laves phases along the lath boundary, and could exist independently at the lath boundary with many dislocations (Fig. 16). A three-dimensional atomic probe (3DAP) was used to characterize the different ages of the Cu in the G115 steel matrix. The results showed that

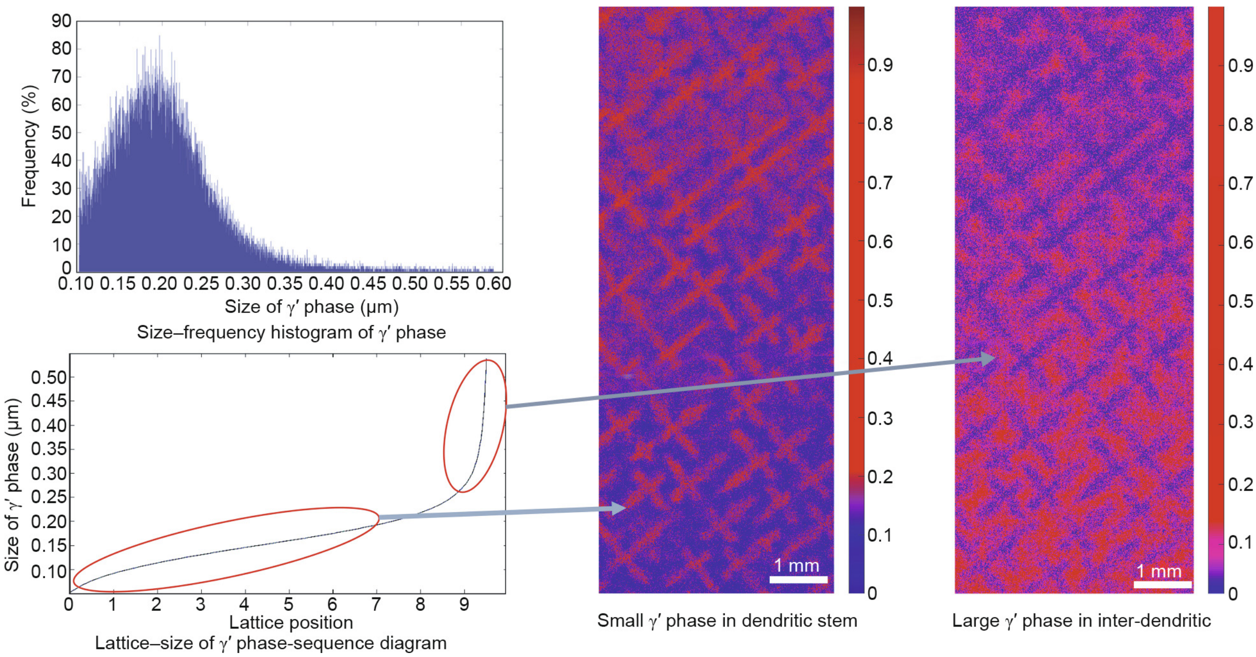

Fig. 11. Distribution γ′-phase grains of different sizes [154].

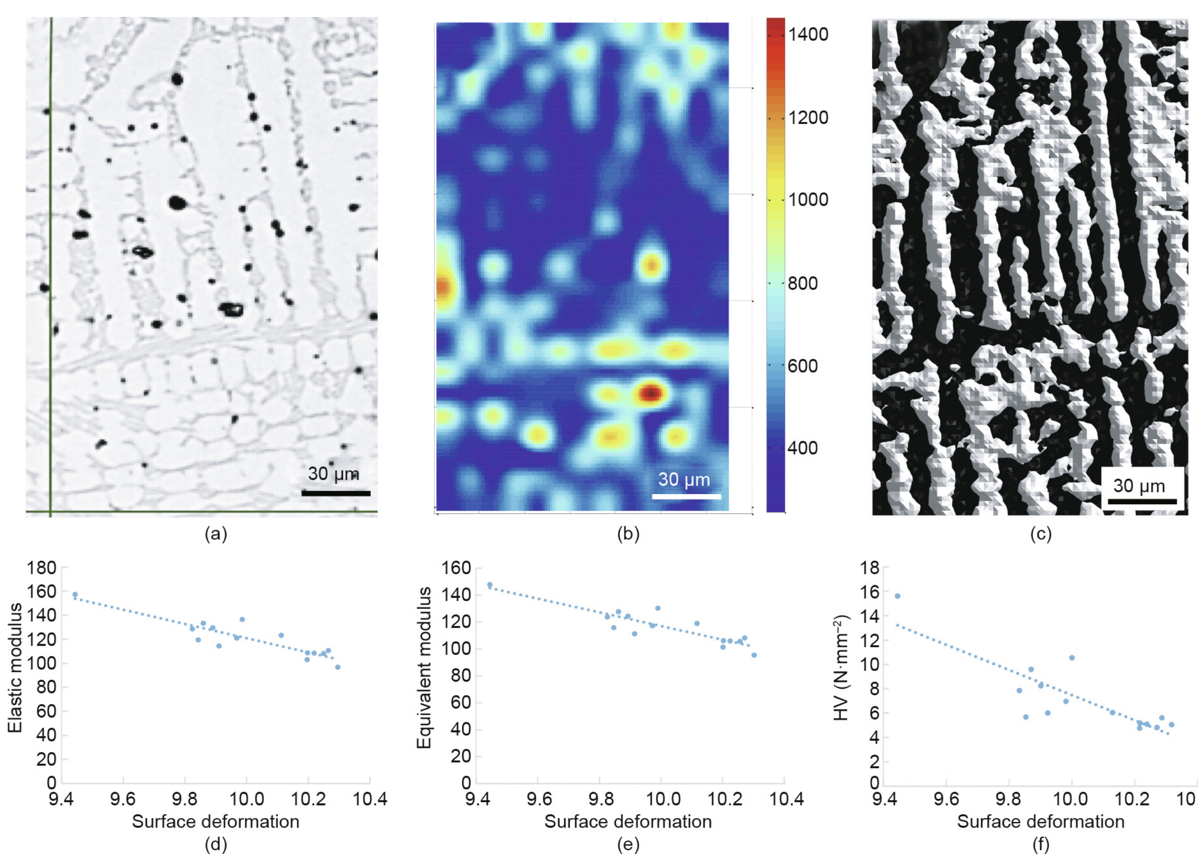

Fig. 12. Study of high-Cr white cast iron by fluid-microprobe-OPA technology [155]. (a) Metallographic structure; (b) microhardness distribution; (c) distribution of isostatic pressure-induced deformation; (d) correlation between elastic modulus and deformation; (e) correlation between equivalent modulus and deformation; (f) correlation between HV and deformation.

a prolonged aging time facilitated Cu precipitation (Table 2). High-throughput statistical spatial-mapping characterization was used to locate and screen from the macroscopic to the microscopic areas, to achieve a high-resolution characterization of the existing form and a distribution of genetic units that contain Cu characteristics, and to reveal the evolution of Cu through a systematic characterization of Cu during the aging of G115 steel (Fig. 17).

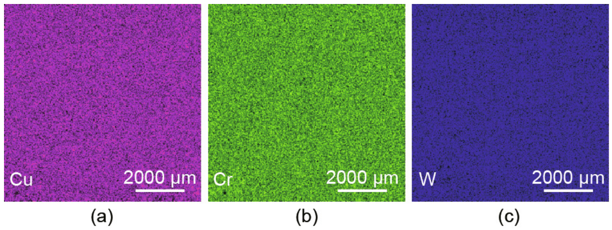

Fig. 13. Characterization of the mesoscopic-to-macroscopic across-scale span distribution of μXRF-OPA technology [156]. (a) μXRF distribution of Cu; (b) μXRF distribution of Cr; (c) μXRF distribution of W.

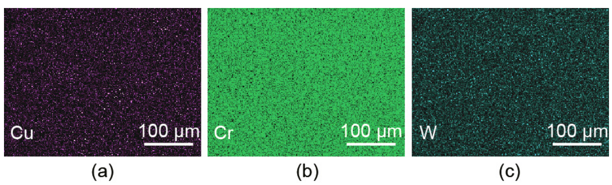

Fig. 14. Characterization of microscopic-to-mesoscopic across-scale span distribution under 1000× magnification of EDS-SEM [156]. (a) SEM distribution of Cu; (b) SEM distribution of Cr; (c) SEM distribution of W.

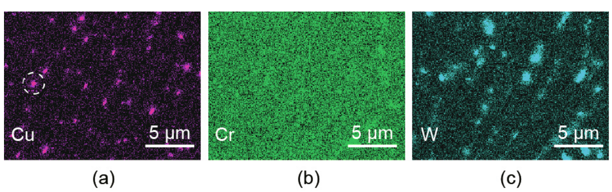

Fig. 15. Characterization of microscopic-to-mesoscopic across-scale span distribution with 20 000× magnification of EDS-SEM [156]. (a) SEM distribution of Cu; (b) SEM distribution of Cr; (c) SEM distribution of W.

Table 1
STEM-EDS analysis of the characteristic genetic units of Cu in G115 steel [156].

Item	Cu	Fe	Cr	Co	Mn
Content (wt%)	90.28	5.64	2.13	0.50	1.44

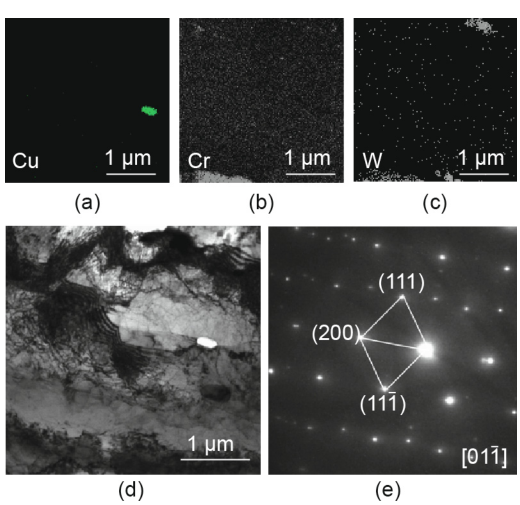

Fig. 16. Characterization of microscopic distribution by STEM [156]. (a) STEM distribution of Cu; (b) STEM distribution of Cr; (c) STEM distribution of W; (d) transmission electron microscopy (TEM) image of Cu; (e) electron diffraction pattern of Cu in selected region.

Table 2
Analysis results of Cu content in the matrix of G115 steel during aging by 3DAP [156].

Item	Cu content in matrix
Tempered	0.48 ± 0.20
650 °C heat treated (equivalent 3000 h)	0.18 ± 0.05
650 °C heat treated (equivalent 8000 h)	0.15 ± 0.03

3.2. Statistical spatial-mapping characterization of the composition, structure, and properties of macroscopic deforming FGH96 turbine disks

Ni-based superalloy is a key material in aeroengines and gas turbine disks, but its modification and optimization in research and development cycles are long. Because its chemical composition is complex, service environments are hostile and performance requirements are strict. Macroscopic deforming FGH96 turbine disks use electroslag remelting continuous directional solidification (ESR-CDS) to prepare ingots and multidirectional and isothermal forging for molding. The mechanical properties of FGH96 turbine disks made by ESR-CDS are similar to those of the powder FGH96 alloy and this deforming alloy still exists in the engineering-development stage. Lu et al. [157,158] characterized slices of macroscopic deforming FGH96 turbine disks using multiple statistical-distribution characterization technologies, including Spark-OPA, FVM-OPA, and SEM-OPA. Data on the distribution of various disk parameters on the disk were obtained, and included various compositions; the total amount of the γ' phase, primary γ' phase, secondary γ' phase, tertiary γ' phase, and particle size of the γ' phase; grain size; carbide phase; microhardness; room-temperature stress and strain; and creep at high temperature (Fig. 18). Statistical mapping with point-to-point correspondence was established for these data. For 0–100 nm, the relative mass fraction of the γ' phase and the atomic fraction of cobalt (Co) and Mo that entered the γ' phase had a significant impact on the creep properties at high temperature. A mathematical model of relevance to the regional statistical mapping was established between the genetic unit of the superalloy γ' phase and the properties of creep at high temperature (Fig. 19), which plays an important role in guiding the modification of superalloy turbine disks.

4. Prospects

High-throughput statistical spatial-mapping characterization is a new technology based on OPA theory, which has led to the development of a series of new methods and new apparatuses with independent intellectual property rights such as Spark-OPA, LIBS-OPA, LA-OPA, μXRF-OPA, FVM-OPA, SEM-OPA, and fluid microprobe-OPA. Many application results have been achieved using high-throughput statistical spatial-mapping characterization technology. Across-scale span high-throughput characterization of composition, structure, and mechanical properties has been realized for all kinds of carbon steel, stainless steel, nonferrous metal, continuous casting slabs, coated plates, superalloy, and heat-resistant steel. In practice, materials, parts, and components in use at the macroscale are inherently non-uniform or heterogeneous in regard to their composition/structure/properties at different scales. The applications of high-throughput experimental tools are extremely useful to fully characterize materials' composition/structure/properties at different scales, and to establish various valuable composition–structure–property relationships. Hence, the seven high-throughput experimental characterization tools presented here, and the composition–structure–property data and relationships that can be obtained through their use, powerfully enable the materials genome engineering methodology.

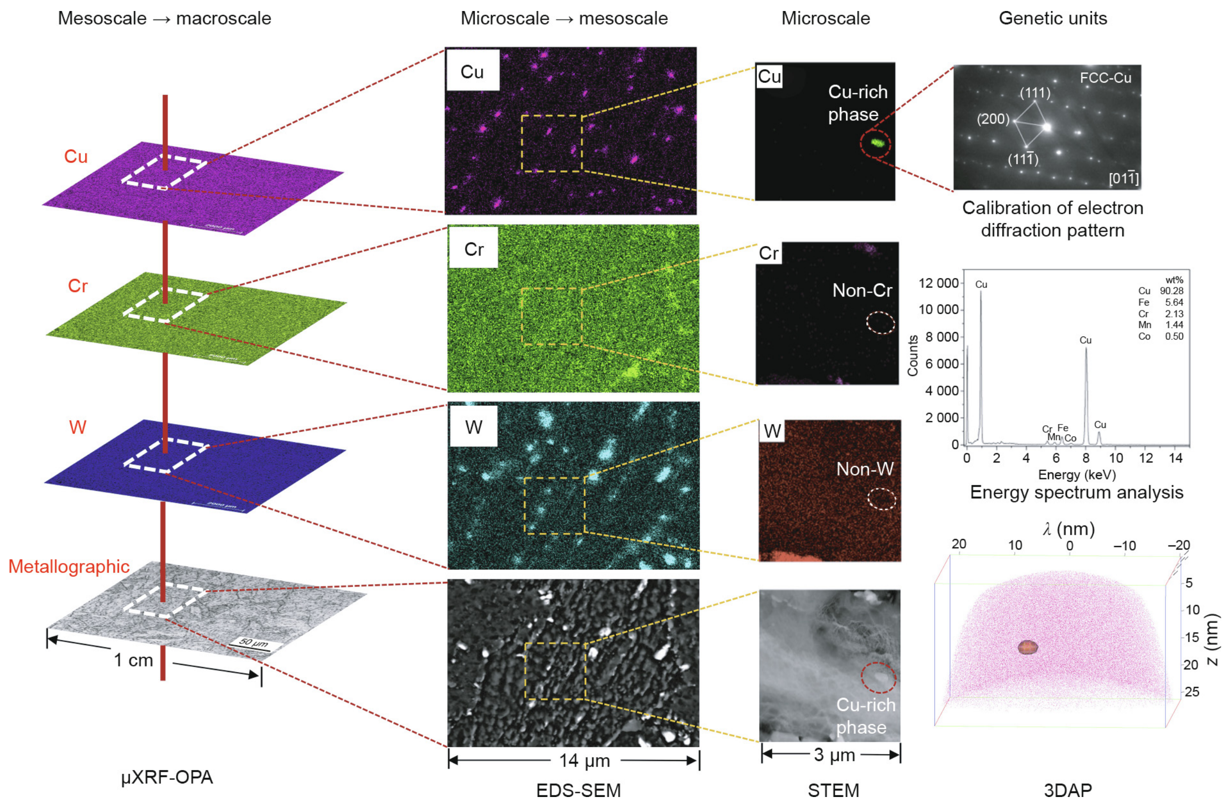

Fig. 17. Characterization of Cu-rich phase in G115 steel by across-scale span high-throughput statistical spatial-mapping [156].

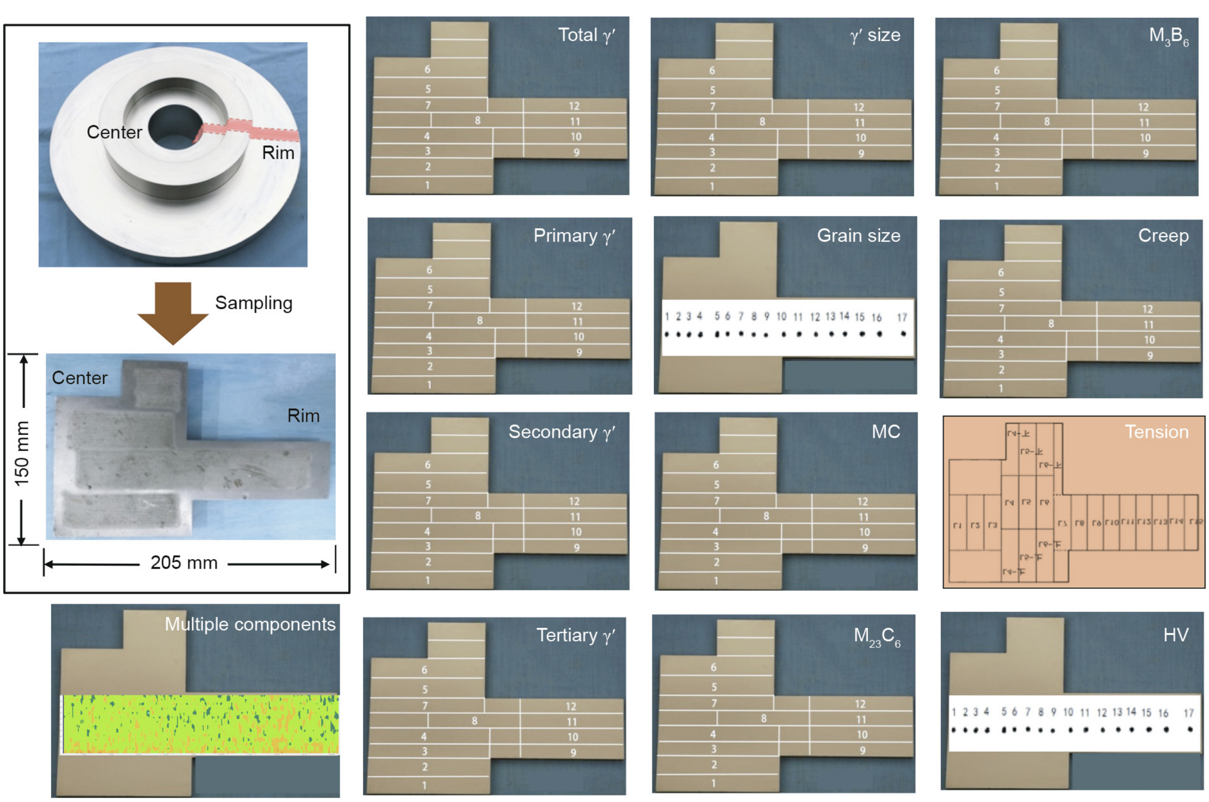

Fig. 18. Characterization of multi-parameter high-throughput statistical distribution. MC, $M_{23}C_6$, and M_3B_6 are type carbides [154].

Through top-down analysis from the macroscale to the microscale, genetic units that affect material properties are screened out, and a model of across-scale span statistical spatial-mapping of the material composition, structure, and properties can be established. The most significant advantage of this method is its similarity to the production process that helps to provide insight into material

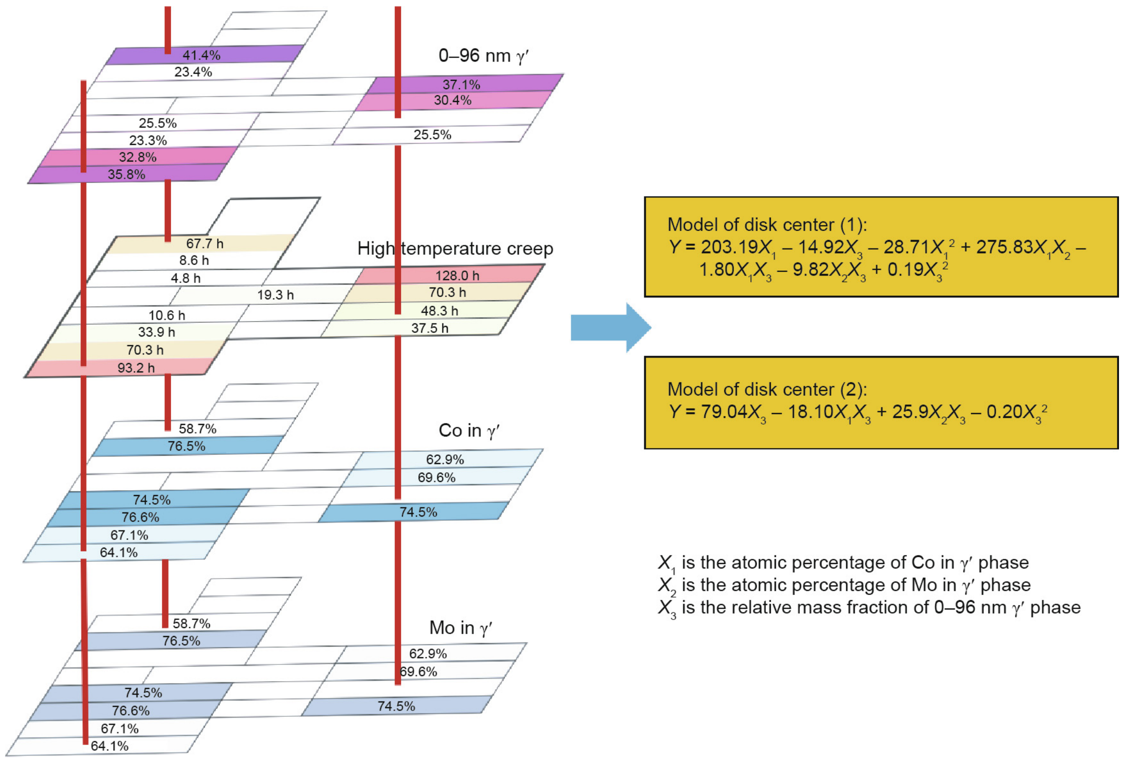

Fig. 19. Mathematical model of the relevance of statistical spatial-mapping between the γ' phase and high-temperature creep.

modification and process optimization. Its disadvantage is that the design-regulated degree of freedom is limited by the process. Future research should focus on the integration of these tools, establish a data analysis process, establish further tools such as machine learning tools, and improve the calibration or coordination of positions while applying two or more characterization tools. Such research would make it possible to reconstruct the high-resolution composition, structure, and properties of the overall macroscopic material at each position and in each microregion, in order to significantly accelerate the discovery and reverse design of new materials.

Acknowledgements

This research was supported by the National Key Research and Development Program of China (2016YFB0700300). The authors acknowledge helpful discussions with Profs. Hong Wang, Xiaodong Xiang, and Liang Jiang. We thank Laura Kuhar, Ph.D. from Liwen Bianji, Edanz Group China (www.liwenbianji.cn/ac), for editing the English text of a draft of this manuscript.

Compliance with ethics guidelines

Haizhou Wang, Lei Zhao, Yunhai Jia, Dongling Li, Lixia Yang, Yuhua Lu, Guang Feng, and Weihao Wan declare that they have no conflicts of interest or financial conflicts to disclose.

Appendix A. Supplementary data

Supplementary data associated with this article can be found in the online at https://doi.org/10.1016/j.eng.2020.05.005.

References

[1] Xiang XD, Sun XD, Briceño G, Luo YL, Wang KA, Chang HY, et al. A combinatorial approach to materials discovery. Science 1995;268 (5218):1738–40.
[2] Zhao JC, Jackson MR, Peluso LA, Brewer LN. A diffusion multiple approach for the accelerated design of structural materials. MRS Bull 2002;27(4):324–9.
[3] Mao SS. High throughput growth and characterization of thin film materials. J Cryst Growth 2013;379:123–30.
[4] Chen L, Bao J, Gao C, Huang SX, Liu CH, Liu WH. Combinatorial synthesis of insoluble oxide library from ultrafine/nano particle suspension using a drop-on-demand inkjet delivery system. J Comb Chem 2004;6(5):699–702.
[5] Gregoire JM, Dale D, Kazimirov A, DiSalvo FJ, van Dover RB. Cosputtered composition-spread reproducibility established by high-throughput X-ray fluorescence. J Vac Sci Technol A 2010;28(5):1279–80.
[6] Gregoire JM, Dale D, Kazimirov A, DiSalvo FJ, van Dover RB. High energy X-ray diffraction/X-ray fluorescence spectroscopy for high-throughput analysis of composition spread thin films. Rev Sci Instrum 2009;80(12):123905.
[7] Reddington E, Sapienza A, Gurau B, Viswanathan R, Sarangapani S, Smotkin ES, et al. Combinatorial electrochemistry: a highly parallel, optical screening method for discovery of better electrocatalysts. Science 1998;280 (5370):1735–7.
[8] Liu XN, Shen Y, Yang RT, Zou SH, Ji XL, Shi L, et al. Inkjet printing assisted synthesis of multicomponent mesoporous metal oxides for ultrafast catalyst exploration. Nano Lett 2012;12(11):5733–9.
[9] Wei T, Xiang XD, Wallace-Freedman WG, Schultz PG. Scanning tip microwave near-field microscope. Appl Phys Lett 1996;68(24):3506–8.
[10] Oral A, Bending SJ, Henini M. Scanning hall probe microscopy of superconductors and magnetic materials. J Vac Sci Technol B 1996;14 (2):1202–5.
[11] Takeuchi I, Yang W, Chang KS, Aronova MA, Venkatesan T, Vispute RD, et al. Monolithic multichannel ultraviolet detector arrays and continuous phase evolution in $Mg_xZn_{1-x}O$ composition spreads. J Appl Phys 2003;94 (11):7336–40.
[12] Huxtable S, Cahill DG, Fauconnier V, White JO, Zhao JC. Thermal conductivity imaging at micrometre-scale resolution for combinatorial studies of materials. Nat Mater 2004;3(5):298–301.
[13] Kim HJ, Han JH, Kaiser R, Oh KH, Vlassak JJ. High-throughput analysis of thin-film stresses using arrays of micromachined cantilever beams. Rev Sci Instrum 2008;79(4):045112.
[14] Wang HZ, Wang H, Ding H, Xiang XD, Xiang Y, Zhang XK. Progress in high-throughput materials synthesis and characterization. Sci Technol Rev 2015;33(10):31–49.

[15] Wang HZ, Jia YH, Zhao L, Li DL, Zhong ZQ. The combinatorial experiment technique of materials' genetic units reflection mapping characterized by high throughput original position statistic distribution analysis based on the inhomogeneous property of materials. In: Proceedings of the No.195 Chinese Engineering Science and Technology Forum—PFIT'2014; 2014 Oct 19; Beijing, China; 2014. p. 7–8. Chinese.
[16] Wang HZ, Li ML, Zhuang JY. Original position statistic distribution analysis characterization of niobium on the vertical section of casting of superalloypneumatic plate wheel. Eng Sci 2011;13(10):19–27. Chinese.
[17] Liu YH, Wang G, Wang RJ, Zhao DQ, Pan MX, Wang WH. Super plastic bulk metallic glasses at room temperature. Science 2007;315(5817):1385–8.
[18] Yu HB, Shen X, Wang Z, Gu L, Wang WH, Bai HY. Tensile plasticity in metallic glasses with pronounced β relaxations. Phys Rev Lett 2012;108(1):015504.
[19] Ichitsubo T, Matsubara E, Yamamoto T, Chen HS, Nishiyama N, Saida J, et al. Microstructure of fragile metallic glasses inferred from ultrasound-accelerated crystallization in Pd-based metallic glasses. Phys Rev Lett 2005;95(24):245501.
[20] Wang WH. Metallic glasses family traits. Nat Mater 2012;11(4):275–6.
[21] Liu YH, Wang D, Nakajima K, Zhang W, Hirata A, Nishi T, et al. Characterization of nanoscale mechanical heterogeneity in a metallic glass by dynamic force microscopy. Phys Rev Lett 2011;106(12):125504.
[22] Wagner H, Bedorf D, Küchemann S, Schwabe M, Zhang B, Arnold W, et al. Local elastic properties of a metallic glass. Nat Mater 2011;10(6):439–42.
[23] Peng HL, Li MZ, Wang WH. Structural signature of plastic deformation in metallic glasses. Phys Rev Lett 2011;106(13):135503.
[24] Hassani M, Lagogianni AE, Varnik F. Probing the degree of heterogeneity within a shear band of a model glass. Phys Rev Lett 2019;123(19):195502.
[25] Wang HZ, Chen JW, Yang ZJ, Yang XS, Gao HB, Jia YH, et al. Research of original position statistic distribution analysis technique. In: Proceedings of the Development of Science and Technology Awards of China Association for Instrumental Analysis; 2015 Oct 27–29; Beijing, China; 2015. Chinese.
[26] Wang HZ. Current state of metallurgical analysis in China and its future trends. Metall Anal 2007;27(1):1–6.
[27] Wang HZ. Original position statistic distribution analysis (OPA)—novel statistic characterization method of different chemical compositions and its states of the materials. Mater Sci Forum 2007;539–543:4446–51.
[28] Wang HZ. A new method of statistic characterization of specific properties of materials—original position statistic distribution analysis. Phys Test Chem Anal Part B Chem Anal 2006;42(1):1–5.
[29] Wang HZ. Original position statistic distribution analysis—new analytical method in quality evaluation of process metallurgy and metal materials. Chin J Nonferrous Met 2004;S1:98–105.
[30] Wang HZ. Original position statistic distribution analysis (original position analysis)—a new analytical method in research and quality evaluation of materials. Sci China Ser B 2003;46(2):119–23.
[31] Wang HZ, Yang ZJ, Chen JW, Yang XS. Original position statistic distribution analysis system. China Metall 2002;6:23–5. Chinese.
[32] Wang HZ. Original position statistic distribution analysis-new technology of material research and quality criterion. Sci China Ser B 2002;32(6):481–5. Chinese.
[33] Chen JW, Yang XS, Chang LL, Hu Y, Yuan LJ, Wang HZ. Development of original position analyzer for metal. Mod Sci Instrum 2005;5:14–7.
[34] Wang HZ, Chen JW, Yang ZJ, Yang XS, Gao HB, Jia YH, et al., inventors; Central Iron & Steel Research Institute, assignee. Original position statistic distribution analysis method. China patent CN200210053706.1. 2004 Jun 16. Chinese.
[35] Wang HZ, Chen JW, Yang ZJ, Yang XS, Gao HB, Jia YH, et al., inventors; Central Iron & Steel Research Institute, assignee. Original position analyzer for metal. China patent CN200210053707.6. 2004 Jun 16. Chinese.
[36] Wang HZ, Yang XS, Zhang XX, Peng XY, Li ML, Chen YY, et al., inventors; NCS Testing Technology Co. Ltd., assignee. Suspension scanning method and sample fixture of original position analyzer for metal. China patent CN200510123305.2. 2006 May 3. Chinese.
[37] Wang HZ, Chen JW, Yang ZJ, Yang XS, Gao HB, Jia YH, et al., inventors; Central Iron & Steel Research Institute (CN), assignee. A method for analysing metals in the fundamental state utilizing the statistical distribution of elements. Europe patent EP2003009038. 2003 Oct 22.
[38] Wang HZ, Chen JW, Yang ZJ, Yang XS, Gao HB, Jia YH, et al., inventors; Central Iron & Steel Research Institute (CN), assignee. Analyzer for metal. Europe patent EP20030007171. 2003 Oct 8.
[39] Wang HZ, Chen JW, Yang ZJ, Yang XS, Gao HB, Jia YH, et al., inventors; NCS Testing Technology Co. Ltd., assignee. Methode d'analyse de distribution statistique de position originale pour un metal. France patent FR2838827 (A3). 2003 Feb 19.
[40] Wang HZ, Zhang XX, Jia HY, Chen JW, Zhao X, Li ML, inventors; Central Iron & Steel Research Institute, assignee. Original position statistical distribution analysis of inclusion size in metal materials. China patent CN200410090616.9. 2005 Apr 27. Chinese.
[41] Ministry of Science and Technology of the People's Republic of China. Original-position statistical distribution analysis of metal. National Technological Invention Award in 2008. No. F-215-2-01. Chinese.
[42] Zuo XJ, Cheng GG, Li J. Original position statistic distribution analysis of the continuous casting billet of 20MnSi steel. Metall Anal 2018;38(1):9–15. Chinese.
[43] Zuo XJ, Du S, Liu Q, Cheng HJ, Li J. Original position statistic distribution analysis of the elements in cross section of pipe line steel continuous casting slab. Metall Anal 2017;37(1):1–7. Chinese.
[44] Zhang TT. Original position statistic distribution analysis of pipeline steel continuous casting slab in soft reduction. Metall Anal 2017;37(5):19–24. Chinese.
[45] Zhou LP. Composition distribution characteristics of 450 mm thick continuous casting slab in full thickness. Mod Metall 2017;45(1):1–4. Chinese.
[46] Qin ZQ, Kang ZQ, Lan CH. Original position statistic distribution analysis of central carbon segregation in GCr15 continuous casting billet. Mod Metall 2017;45(1):10–3. Chinese.
[47] Yu ZY, Liu K, Qiu ST, Yan HC, Wang XY. Original position statistic distribution analysis for the continuous casting slab of 72A tire cord steel. Metall Anal 2016;36(12):1–7. Chinese.
[48] Zhou LP. Original position statistic distribution analysis of composition distribution of 200 square continuous casting billet. Mod Metall 2016;44 (2):19–22. Chinese.
[49] Luo QH, Li DL, Fan YZ, Wang HZ. Original position statistic distribution analysis for element segregation of cross-section of stainless steel continuous casting slab. Metall Anal 2015;35(10):1–7. Chinese.
[50] Luo QH, Li DL, Wang HZ. Original position statistic distribution analysis for element segregation of cross-section of stainless steel continuous casting slab. In: Proceedings of the No.195 Chinese Engineering Science and Technology Forum—PFIT'2014; 2014 Oct 19; Beijing, China. p. 186–7. Chinese.
[51] Zhang Z, Liu RQ, Zhu GR, Huang Z, Xu XH. Application of original position statistic distribution analysis in improving central segregation of cord steel. Mod Metall 2014;42(5):24–6. Chinese.
[52] Luo QH. Study on solute migration of stainless steel continuous casting slab during rolling process by original position statistic distribution analysis technique [dissertation]. Beijing: China Iron and Steel Research Institute; 2014. Chinese.
[53] Li JW, Zhang SZ, Xia NP, Yu WH, Li DL. Original position statistic distribution analysis for the large square billet of 82A tire cord steel. Metall Anal 2013;33 (7):1–9. Chinese.
[54] Li DL, Wen ZM, Wang HZ. Original position statistic distribution analysis for the round billet of steel 35. Metall Anal 2012;32(12):1–7. Chinese.
[55] Wang KJ, Li W. Application of original position statistic distribution analysis technique in composition segregation detection of continuous casting slab. Metall Anal 2012;32(1):7–14. Chinese.
[56] Lin ZG, Zhang XF, Zhang JL, Zhang S. Han-Steel Handan iron and steel non-oriented electrical steel H50W800 casting *in-situ* analysis. In: Proceedings of the 8th (2011) China Iron and Steel Annual Conference; 2011 Oct 26; Beijing, China. p. 2489–93. Chinese.
[57] Xia NP, Yu WH, Zhang SZ, Chen SH, Gui JB. Study on central segregation in continuous casting slab of high carbon steel by original position statistic distribution analysis technique. Metall Anal 2011;31(10):1–6. Chinese.
[58] Li ML, Wang H, Yang ZG, Feng XX, Chen JW, Jia YH, et al. Original position statistic distribution analysis of carbon, silicon, manganese, phosphorus, sulfur, niobium, titanium, vanadium in the cross section of different middle and low alloy steel continuous casting slabs. Metall Anal 2011;31(6):1–8. Chinese.
[59] Chen ZR, Shen Z. Application of original position statistic distribution analysis technique in segregation analysis of continuous casting billets. Metall Anal 2010;30(12):1–5.
[60] Li W, Wang KJ. Study on carbon and manganese original position statistical distribution of high carbon continuous cast round billet. Tianjin Metall 2010;(4):16–20,75. Chinese.
[61] Ji YL, Liu JH, Chen F, Liu J. Research on centerline segregation heredity of F550 shipbuilding steel. In: Proceedings of 10th Annual Conference of China Iron and Steel and 6th Annual Academic Conference of Baosteel; 2015 Oct 21; Shanghai, China. p. 663–71. Chinese.
[62] Yuan LJ, Hu P, Shi XX, Wang HZ. Segregation study of carbon in the fracture sample of shipbuilding steel plate by spark source original position statistic distribution analysis technique. Metall Anal 2010;30(7):1–5. Chinese.
[63] Huang YS. Analysis of segregation in imported thick steel plate by original position statistic distribution analysis technique. Metall Anal 2010;30(1):1–6.
[64] Guo HH, Song B, Mao JH, Zhao P. Effect of rare earth elements on macrosegregation in weather-resisting steel. J Univ Sci Technol B 2010;32 (1):44–9,66. Chinese.
[65] Li ML, Wang H, Yang ZG, Wu C, Chen JW, Wang HZ. Distribution analysis of C, Si, Mn, P, S, Nb, Ti, V in the cross section of different low and middle iron and steel continuous casting slabs by OPA technique. In: Proceedings of the 7th (2009) China Iron and Steel Annual Conference; 2009 Nov 11; Beijing, China. p. 1732–9. Chinese.
[66] Wang HZ, Li ML, Zhang XX, Wu C. Original position statistic distribution analysis (OPA) on the quality of mould steel billet. Eng Sci 2009;11 (10):39–47. Chinese.
[67] Li XH, Kang YL, Wu GL, Xiao AD. Original position statistic distribution analysis for thin slab produced by CSP. J Iron Steel Res 2009;21(8):9–12,34.
[68] Li ML, Chen JW, Wu C, Zhang XX, Jia YH, Wang HZ. Segregation analysis of different stainless steel slabs by original position statistic distribution analysis technique. Metall Anal 2008;6:1–10. Chinese.

[69] Chen FQ. Segregation in continuous casting billet and flat-bulb steel of 10CrNiCu and its effect on mechanical properties [dissertation]. Harbin: Harbin Engineering University; 2008. Chinese.
[70] Chen JW, Wang HZ. Study on original position statistic distribution analysis of low alloy steel continuous casting billet. Metall Anal 2007;9:1–6.
[71] Yang ZM, He YT, Lin ST. Original position statistic distribution analysis for automobile beam slab. Metall Anal 2007;7:36–41. Chinese.
[72] Xue ZL, Zuo DW, Qi JH, Gao JB, Jiang DY, Wang GR, et al. Analysis of original position statistic distribution on solidification segregation of cast billet. Spec Steel 2007;1:13–5. Chinese.
[73] Yuan LJ, Wang HZ. Temperature effect and its mathematic correction mode for original position statistic distribution analysis. Metall Anal 2007;6:28–31. Chinese.
[74] Yuan LJ, Wang HZ. Correction of matrix effect for the determination of components in stainless steel by original position statistic distribution analysis. Metall Anal 2006;6:20–2. Chinese.
[75] Liu J. Original position statistic distribution analysis for radial steel billet. Henan Metall 2006;(S2):24–26,49. Chinese.
[76] Xue ZL, Qi JH, Gao JB, Zuo DW, Jiang DY, Wang GR, et al. Study on solidification segregation of billets based on original position statistic distribution analysis. Henan Metall 2006;(S2):36–9. Chinese.
[77] Yang YJ. Application of original position statistic distribution analysis technique in analysis of continuous casting billets [dissertation]. Changsha: Central South University; 2006. Chinese.
[78] Wang HZ, Zhao P, Chen JW, Li ML, Yang ZJ, Wu C. Original position statistic distribution analysis study of low alloy steel continuous casting billet. Sci China Ser E 2005;48(1):104–15.
[79] Wang HZ, Li ML, Chen JW, Wu C. Original position statistic distribution analysis (OPA) study on the quality of billet. Eng Sci 2003;10:34–42. Chinese.
[80] Yang ZJ, Wang HZ. Application research of original position analysis for quality control of C-C billets. In: Proceedings of the 7th Beijing Youth Science and Technology Papers Selection Award-winning Papers Collection; 2003 Dec; Beijing, China; 2003. p. 185. Chinese.
[81] Yang ZJ, Wang HZ. Original position analysis for low alloy steel billets with different microstructure. Iron Steel 2003;38(9):67–71. Chinese.
[82] Li DL, Gao Y, Wen ZM, Wang HZ. Original position statistical distribution characterization of high-quality carbon structural steel round billet and its relationship with microstructure and mechanical properties. Min Metall 2013;22(S1):107–11. Chinese.
[83] Wang WL. Discriminant quality defects of aluminum alloys and three others by original position analysis [dissertation]. Beijing: General Research Institute for Nonferrous Metals; 2013. Chinese.
[84] Wang WL, Zhang XX, Liu Y, Liu J, Tong J, Zhang Y, et al. Original position statistic distribution analysis of casting brass. Metall Anal 2013;33(6):1–8. Chinese.
[85] Li DL, Cheng HM, Si H, Zhang Y, Wang HZ. Original position statistic distribution analysis for aluminum/silicon casting aluminum alloys. Metall Anal 2012;32(10):37–44. Chinese.
[86] Zhao L, Jia YH, Liu QB, Chen JW, Wang HZ. Determination of inclusion single manganese content in iron and steel with discharge analysis. Metall Anal 2006;(1):1–5. Chinese.
[87] Li DL, Si H, Li ML, Jia YH, Wang HZ. Determination of particle size of silicon inclusions in steel by original position statistic distribution analysis technique. Metall Anal 2009;29(1):1–7. Chinese.
[88] Liu G, Jia YH, Chen JW, Wang HZ. Study on the spectroscopic behavior of TiN and TiC in steel. Metall Anal 2003;3:25–7. Chinese.
[89] Yang ZJ, Wang HZ. Research on segregation and inclusion of continuous casting slab by original position analysis. Iron Steel 2003;(3):61–3. Chinese.
[90] Zhang TT. Analysis of manganese sulfide inclusion size distribution in heavy rail steel by original position statistic distribution technique. Metall Anal 2017;37(7):6–10. Chinese.
[91] Li DL, Gao HB, Li ML, Qu WJ, Zhang XX, Jia YH, et al. A new original position analysis method for inclusion size in high performance alloy structural steel. In: Proceedings of the 2015 Conference of China Association for Instrumental Analysis; 2015 Jul; Beijing, China; 2015. Chinese.
[92] Li DL, Xia NP, Li JW, Zhang SZ, Yu WH. Original position statistic distribution analysis method for inclusions in beam steel. Metall Anal 2014;34(12):1–6. Chinese.
[93] Li DL, Li JW, Zhang SZ, Xia NP, Yu WH. Study on original position statistic quantitative method for the content of aluminium inclusions in steel. Metall Anal 2014;34(3):1–6. Chinese.
[94] Li DL, Wang HZ. Original position statistic distribution analysis for the sulfides in gear steels. ISIJ Int 2014;54(1):160–4.
[95] Liu JH, Bao YP, Wang GX, Yang Y, Li KM, Li LX. Investigation of inclusion distribution in ingots of high pressure boiler-tube steel P12 by dissection. J Univ Sci Technol B 2012;34(7):769–74. Chinese.
[96] Li DL, Xiao GH, Jia YH, Wang HZ. Original position statistical distribution analysis of sulfide in gear steel. In: Proceedings of 2nd Steel Quality Control Technology Conference; 2012 Mar 2; Beijing, China. p. 185–93. Chinese.
[97] Li DL, Li ML, Jia YH, Wang HZ. Application of spark source atomic emission spectrometry to the state analysis of inclusions in steel. Metall Anal 2011;31 (5):20–6. Chinese.
[98] Li DL, Li ML, Jia YH, Wang HZ. Quantitative analysis of silicon inclusions in steel by original position statistic distribution analysis technique. Metall Anal 2011;31(1):1–6. Chinese.
[99] Gong YY, Han CM. Statistic dispersion analysis of inclusions in continuous casting round billet. In: Proceedings of 7th (2009) China Iron and Steel Annual Conference; 2009 Nov 11; Beijing, China. p. 916–9. Chinese.
[100] Li ML, Gao HB, Chang LL, Yuan LJ, Wang HZ. Original position statistic distribution analysis of manganese, titanium, aluminium, niobium inclusions in stainless steel slabs. Metall Anal 2009;29(6):1–6. Chinese.
[101] Gao HB, Jia YH, Li ML, Yuan LJ, Wang HZ. Research on original position statistic distribution analysis model for grain size of aluminium inclusion in steel. Metall Anal 2009;29(5):1–5. Chinese.
[102] Zhang XX, Jia YH, Chen JW, Li DL, Wang HZ. Size determination of aluminium inclusions in steel by original position statistic distribution analysis technique. Metall Anal 2009;29(4):1–6. Chinese.
[103] Li DL, Zhou W, Li ML, Jia YH, Wang HZ. State analysis of inclusions in rectangular casting blank. Metall Anal 2007;11:1–6.
[104] Yao NJ, Chen JW, Yang ZJ, Wang HZ. Laser-induced breakdown spectrometer—a new tool for quick analysis of on-the-spot sample in metallurgy. Spectrosc Spect Anal 2007;7:1452–4.
[105] Wang H, Jia YH. Original position statistic distribution analysis of aluminum inclusion in middle-low alloy steel. Metall Anal 2007;8:1–4. Chinese.
[106] Zhang XX, Jia YH, Chen JW, Li ML, Wang HZ. The criterion of original position statistic distribution analysis for the aluminum inclusion in steel. Metall Anal 2006;4:1–4. Chinese.
[107] Chen JW, Li ML, Wu C, Zhang XX, Wang HZ, Yang CZ, et al. Original position statistic distribution analysis of the centerline segregation and the inclusion distribution in the cross section of continuous casting slab under different drawing speed technology conditions. Metall Anal 2006;3:1–6. Chinese.
[108] Luo QH, Li DL, Ma FC, Yang C, Wang HZ. Original position statistic distribution analysis for inclusion of cross-section of stainless steel continuous casting slab. Metall Anal 2013;33(12):1–7. Chinese.
[109] Zhang Y, Jia YH, Chen JW, Shen XJ, Liu Y, Zhao L, et al. Comparison of the analytical performances of laser-induced breakdown spectroscopy and spark-OES. ISIJ Int 2014;54(1):136–40.
[110] Zhang Y, Jia YH, Chen JW, Shen XJ, Zhao L, Yang C, et al. Study on parameters influencing analytical performance of laser-induced breakdown spectroscopy. Front Phys 2012;7(6):714–20.
[111] Chen JW, Zhao L, Yao NJ, Han PC, Yuan LJ, Chen YY, et al. Original position statistic distribution analysis by laser induced breakdown spectroscopy. In: Proceedings of the CETAS 2011 8th International Workshop on Progress in Analytical Chemistry and Materials Characterisation in the Steel and Metal Industries; 2011 May 17–19; Luxembourg, Luxembourg; 2011.
[112] Wang HZ, Yuan LJ, Jia YH, Chen JW, Chen YH, Shi XX, et al. inventors; NCS Testing Technology Co. Ltd., assignee. Original position statistical distribution analysis method for nonflat surface of materials. China patent CN201010253907.0. 2011 Jan 19. Chinese.
[113] Jia YH, Chen JW, Zhang Y, Li DL, Chen YY, Yang C, et al., inventors; NCS Testing Technology Co. Ltd., assignee. An instrumental analysis method for rapid determination of inclusion content in materials. China patent CN201410013193.4. 2014 Apr 16. Chinese.
[114] Yao NJ, Chen JW, Yang ZJ, Shen XJ, Wang HZ, inventors; NCS Testing Technology Co. Ltd., assignee. A focusing device of laser ablation for microregion analysis. China patent CN200610057540.9. 2006 Aug 9. Chinese.
[115] Yao NJ, Yang ZJ, Shen XJ, Wang HZ, Luo QH, Cheng HM, inventors; Central Iron & Steel Research Institute, assignee. A solid sampling device of laser ablation. China patent CN200620007911.8. 2006 Mar 14. Chinese.
[116] Li DL, Yang LX, Lu YH, Zhu YJ. Statistic distribution characterization of compositions, microstructure and microhardness in surfacing area. J Iron Steel Res 2018;30(2):139–43. Chinese.
[117] Yang C, Zhang Y, Jia YH, Wang HZ. Element distribution analysis of welded fusion zone by laser-induced breakdown spectroscopy. Spectrosc Spect Anal 2014;34(4):1089–94. Chinese.
[118] Li DL, Zhang Y, Wang HZ, Miao RY. Original opposition statistic distribution analysis combined with laser induced breakdown spectrometry for metal gadolinium. J Chin Rare Earth Soc 2014;32(1):76–83. Chinese.
[119] Li DL, Jin C, Ma FC, Zhang Y, Wang HZ. Original position statistic distribution analysis combined with laser induced breakdown spectrometry for the element segregation in tire cord steel rod. Metall Anal 2014;34(1):1–9. Chinese.
[120] Zhang Y, Jia YH, Chen JW, Shen XJ, Zhao L, Li DL, et al. Segregation bands analysis of steel sample using laser-induced breakdown spectroscopy. Spectrosc Spect Anal 2013;33(12):3383–7. Chinese.
[121] Qu HY, Hu JY, Zhao L, Han PC, Chen YY, Liu J, et al. Determination of nine elements iron and steel samples with surface oxidization by laser induced breakdown spectroscopy. Metall Anal 2012;32(7):1–6. Chinese.
[122] Yuan LJ, Shi XX, Lian ZQ, Zhang SK. Study on the improvement of analysis precision for laser induced breakdown spectrometry. Metall Anal 2012;32 (2):1–5. Chinese.
[123] Shao HQ, Ruan Q, Liu Y, Yang C, Liu JM, Jia YH. Analysis of strip defect on the surface of cold-rolled hot dipped galvanized sheet and discussion on the cause of formation. Metall Anal 2015;35(4):1–7.
[124] Chen JW, Zhao L, Han PC, Yuan LJ, Qu HY, Chen YY, et al. A new LIBS-OPA method for defects of surface-treated materials such as advanced automotive steel plates. In: Proceedings of the Development of Science and Technology

Awards of China Association for Instrumental Analysis Conference; 2015 Jul; Beijing, China; 2015. Chinese.
[125] Qu HY, Hu JY, Zhao L, Han PC, Shen XJ, Yuan LJ, et al. Determination of abnormal elements of linear defects of automobile body sheets by laser induced breakdown spectroscopy-original position statistic distribution analysis technique. Metall Anal 2013;33(1):1–6. Chinese.
[126] Zhao L, Han PC, Yuan LJ, Qu HY, Chen YY, Yao NJ, et al. Laser induced breakdown spectroscopy-original position statistic distribution analysis technique. In: Proceedings of the 2nd Conference on Steel Quality Control Technology-Shape, Performance, Dimensional Accuracy, Surface Quality Control and Improvement; 2012 Mar 2; Beijing, China. Beijing: The Chinese Society for Metals, Beijing Mechanical Engineering Society; 2012. p. 401–7. Chinese.
[127] Yang C, Jia YH, Wang H, Li DL, Qu HY, Shen XJ, et al. Statistical analysis of relation of manganese sulfide inclusion area to signal intensity by laser-induced breakdown spectroscopy. Chin J Anal Chem 2018;46(2):265–72. Chinese.
[128] Yang C. Statistical characterization of MnS inclusion in steel by laser-induced breakdown spectroscopy [dissertation]. Beijing: China Iron and Steel Research Institute; 2017. Chinese.
[129] Yang C, Jia YH, Zhang Y. Determination of acid-insoluble aluminum content in steel by laser-induced breakdown spectroscopy. Spectrosc Spect Anal 2015;35(3):777–81. Chinese.
[130] Yang C, Jia YH, Chen JW, Li DL, Liu J, Zhang Y. Characterization of inclusion type in steel by laser-induced breakdown spectroscopy. Chin J Anal Chem 2014;42(11):1623–8. Chinese.
[131] Han M, Zhang X, Hu JY. Correlation discussion between material properties and chemical components in high-strength steel welding joint by original position distribution analysis of laser ablation inductively coupled plasma mass spectrometry. Metall Anal 2018;38(3):1–7. Chinese.
[132] Yang LX, Li DL, Zhang XW, Miao RY, Li XJ. Preliminary exploration on statistical distribution analysis of dysprosium rod by laser ablation-inductively coupled plasma mass spectrometry. Metall Anal 2017;37(5):1–11. Chinese.
[133] Yang LX, Chen J, Song QW, Li DL, Jia SJ, Li XJ. Study on distribution analysis method in crack zone of pipeline steel by laser ablation-inductively coupled plasma mass spectrometry. Metall Anal 2017;37(4):1–9. Chinese.
[134] Wang MH, Han M, Luo QH, Yang GW. Fractionation effect of laser ablation-inductively coupled plasma mass spectrometric determination of trace elements in superalloy and its calibration. Metall Anal 2014;34(7):1–6. Chinese.
[135] Zhao L, Jia YH, Yuan LJ, Chen YH, Qu HY, Zhang Y, et al. Original position statistic distribution analysis characterization technique for composition and state on non-planar surface of materials. Metall Anal 2013;33(4):1–12. Chinese.
[136] Luo QH, Yang C, Wang HZ. Original position statistic distribution analysis on the cross section of stainless steel sheet by laser ablation ICP-MS. In: Proceedings of the 9th China Iron and Steel Annual Conference; 2013 Oct 23; Beijing, China. p. 3689–99. Chinese.
[137] Luo QH, Chen YH, Wang HZ. Determination of seventeen elements in stainless steels by laser ablation inductively coupled plasma mass spectrometry. Metall Anal 2013;33(9):1–7. Chinese.
[138] Yuan LJ, Gao JS, Han GQ, Wang LP, Wang HZ. Characterization of laser ablation inductively coupled plasma mass spectrum-original position statistic distribution analysis of chemical composition in the fracture of low alloy steel. Metall Anal 2012;32(5):1–9. Chinese.
[139] Han M, Hu JY, Wang MH, Wang HZ. Application of laser ablation inductively coupled plasma mass spectrometry to distribution analysis of elements in low alloy steel welding line. Metall Anal 2011;31(8):1–5. Chinese.
[140] Han M, Hu JY, Chen YH, Wang HZ. Determination of trace elements in nickel-base superalloy by laser ablation inductively coupled plasma mass spectrometry with correction of aggregated reference material chips. Metall Anal 2010;30(3):1–6. Chinese.
[141] Yuan LJ, Yu L, Han M, Wang HZ. Original position statistic distribution analysis of impact fracture surface of medium and low alloy steel by laser ablation inductively coupled plasma mass spectrometry. Metall Anal 2010;30(6):1–6. Chinese.
[142] Yuan LJ, Han M, Yu L, Wang HZ. The original position statistic distribution analysis with LA-ICP-MS method for mini-size sample. In: Proceedings of the 7th China Iron and Steel Annual Conference; 2009 Nov 11; Beijing, China. p. 1697–702. Chinese.
[143] Yuan LJ, Hu P, Wang HZ. The original position statistic segregation distribution analysis method for mini-size low alloy steel sample. In: Proceedings of the 7th China Iron and Steel Annual Conference; 2009 Nov 11; Beijing, China. p. 1740–4. Chinese.
[144] Han M, Hu JY. Progress of laser ablation inductively coupled plasma mass spectrometry and its application. In: Proceedings of the 7th China Iron and Steel Annual Conference; 2009 Nov 11; Beijing, China. p. 1703–9. Chinese.
[145] Chen YH, Yuan LJ, Wang HZ. Investigation on original statistic distribution analysis of flat-bulb steel by laser ablation inductively coupled plasma mass spectrometry. Metall Anal 2009;29(9):1–5. Chinese.
[146] Chen YH, Wang HZ. Investigation on sample preparation and quantitative method for analysis of small-scale iron, steel and alloy by laser ablation inductively coupled plasma mass spectrometry. Metall Anal 2009;29(2):1–7. Chinese.
[147] Chen YH, Wang HZ. Influence factors and evaluation of elemental fractionation in laser ablation inductively coupled plasma mass spectrometry. Metall Anal 2008;28(8):1–6. Chinese.
[148] Wang HZ, Chen JW, Yuan LJ, Yu X, Li HW, Li M, et al., inventors; NCS Testing Technology Co. Ltd., assignee. Laser ablation inductively coupled plasma mass spectrometry original position analysis system. China patent CN201110302956.3. 2012 Mar 14. Chinese.
[149] Wang HZ, Chen YH, Luo QH, Jia YH, Gao HB, Li XJ, et al., inventors; China NIL Research Center for Proficiency Testing, assignee. Collective metallurgical standard samples for minimal invasive analysis and their preparation and application. China patent CN200810225865.2. 2009 Apr 1. Chinese.
[150] Zhao L, Wang HZ. Original position statistic distribution analysis for composition and state on non-flat surface of materials. In: Proceedings of the CETAS/Jernkontoret Nordic Chemists' and Metallographers' Technical Meeting; 2012 Nov 28–29; Stockholm, Sweden; 2012.
[151] Yang LX, Zhao L, Li DL, Wang HZ. Multiscale analysis of Cu in 9Cr-3W-3Co martensitic heat resistant steels for ultra-supercritical power plants by micro-XRF/EDS on SEM. In: Proceedings of the 65th Annual Conference on Applications of X-ray Analysis; 2016 Aug 1–5; Denver, CO, USA; 2016.
[152] Li DL, Zhao L, Yang LX, Wang HZ. Content distribution analysis of Nb, Ti, Mo, W in superalloys by high-resolution XRF scanning method. In: Proceedings of the 65th Annual Conference on Applications of X-ray Analysis; 2016 Aug 1–5; Denver, CO, USA; 2016.
[153] Wang HZ, Jia YH, Zhao L, Li DL, Zhong ZQ. High throughput original position statistic reflection mapping. In: Proceedings of the Asia Steel International Conference 2015; 2015 Oct 5–8; Yokohama, Japan; 2015.
[154] Wang HZ, Jia YH, Zhao L, Li DL, Zhong ZQ. High throughput statistic reflection mapping characterization technique based on the non-uniformity nature of materials and its application in the nickel-based superalloys. In: Proceedings of the 2nd Forum on Materials Genome Engineering of Chinese Academy of Engineering; 2018 Oct 14–16; Beijing, China; 2018.
[155] Feng G, Qin HL, Jia YH, Zhao L, Zou YM, Wang SB, et al. Contour map of nano-mechanical-properties using isostatic pressing. Scr Mater 2017;137:69–72.
[156] Yang LX. Multi-scale characterization of Cu and correlation study on composition–structure–properties of ultra supercritical heat resistant steel G115 [dissertation]. Beijing: China Iron and Steel Research Institute; 2017. Chinese.
[157] Lu YH, Shen XJ, Li J, Liu QB, Fu R, Wang P. Physical and chemical phase analysis of turbine disk of wrought FGH96. Metall Anal 2018;38(1):1–8. Chinese.
[158] Lu YH, Wang P, Shen XJ, Fu R, Li FL, Li DL, et al. Characterization of relationship between grain size and hardness of large-size deformation FGH96 superalloy turbine disk. Phys Test Chem Anal Part A 2017;53(8):544–7. Chinese.